ESD-TR-75-283

Technical Note

1975-34

B. E. White

On the Close Packing of Unsynchronized FDM Waveforms

14 October 1975

Prepared for the Department of the Navy
under Electronic Systems Division Contract F19628-76-C-0002 by

Lincoln Laboratory
MASSACHUSETTS INSTITUTE OF TECHNOLOGY
LEXINGTON, MASSACHUSETTS

The work reported in this document was performed at Lincoln Laboratory, a center for research operated by Massachusetts Institute of Technology. The work was sponsored by the Department of the Navy under Air Force Contract F19628-76-C-0002.

This technical report has been reviewed and is approved for publication.

FOR THE COMMANDER

Eugene C. Raabe

Eugene C. Raabe, Lt. Col., USAF
Chief, ESD Lincoln Laboratory Project Office

MASSACHUSETTS INSTITUTE OF TECHNOLOGY

LINCOLN LABORATORY

ON THE CLOSE PACKING OF UNSYNCHRONIZED FDM WAVEFORMS

B. E. WHITE

Group 67

TECHNICAL NOTE 1975-34

14 OCTOBER 1975

LEXINGTON MASSACHUSETTS

ABSTRACT

The effects of crosstalk on unsynchronized FDM communication links operating in the presence of additive white Gaussian noise are considered for several modulation schemes. Continuous-phase frequency shift keying is found to be far superior to various forms of phase shift keying in the sense that many more uncoordinated frequency division multiplexed waveforms can be packed into a given bandwidth for a certain imbalance in transmitter powers. This result can be applied to the uplinks and/or downlinks of a demodulating communications satellite serving a multitude of mobile terminals.

TABLE OF CONTENTS

I. INTRODUCTION AND SUMMARY

The effects of crosstalk on unsynchronized FDM communication links operating in the presence of additive white Gaussian noise (AWGN) are considered in this report. It is shown that continuous-phase binary frequency shift keyed (MSK) modems are superior to binary phase shift keyed (BPSK) or any of the several variants of quadriphase shift keyed (QPSK) modems in the sense that many more frequency division multiplexed (FDM) waveforms can be packed into a given bandwidth at a fixed level of crosstalk interference. This result has particular application to a tactical communications system involving a processing, i.e., demodulating, satellite and a frequency division multiple access (FDMA) uplink and/or an FDM downlink serving large numbers of mobile terminals.

1.1 Background

Consider the problem of providing efficient communications service to hundreds of mobile terminals located just about anywhere on the earth's surface [1]. A reasonable economic balance is attainable with low-cost terminals and a relatively more complex satellite.

This generally implies uncoordinated low-power terminals equipped with ultra-high frequency (UHF) antennas operating with a mixture of data rates and a satellite that tracks the Doppler, if necessary, and symbol timing of each user being demodulated. For a greater degree of standardization, while maintaining a certain flexibility, many terminals could employ 2400 bps vocoded voice or handle data traffic at either a 2400 bps or 75 bps rate, and many others could use 16 kbps continuously variable slope delta (CVSD) modulation voice. In order to provide selected service to several coverage areas simul-

taneously the satellite could employ a multiple beam antenna and an earth coverage antenna to receive communication requests utilizing a demand access mode of operation. In addition to demodulating uplink data and reorganizing this data for the downlink, the satellite obviously would have multifarious control functions to perform.

An FDMA rather than time division multiple access (TDMA) mode* is more appropriate for the uplink considering the high density of frequency allocations at UHF and the lesser ability of weaker terminals to synchronize and support communications at the faster signaling rates dictated by a TDMA format. A code division multiple access (CDMA) technique would also require more interuser cooperation, e.g., power control, than is economically attractive. Thus, the uplink bandwidth would typically consist of several sub-bands each no more than several tens of kHz or a few hundred kHz wide. The downlink bandwidth can be thought of as either a small number of bands several hundred kHz wide for TDM signaling or a segmented arrangement like the uplink for FDM signaling. The total throughput data rate for the satellite would be several hundred kbps.

The extra system complexities implied by imposing transmitter power, timing or Doppler control disciplines on the terminals may be feasible, of course. If the terminals were mutually synchronized in symbol timing and Doppler, then orthogonal signaling could be employed and there would be no power control problem, i.e., crosstalk among user signals at the satellite could be avoided entirely. However, for the system concept adopted here, there

---

* Individual FDM accesses could have a TDMA format, however.

will be mutual interference among the received waveforms in addition to the usual channel noise.

The question addressed in this report is: How severe is the crosstalk interference for several modulation and detection schemes known to be optimum in the presence of AWGN? A more difficult question requiring further research would be: What modems yield the least crosstalk among FDM users occupying a given bandwidth?

This report is a companion to another recent study [2] which presumed more terminal and satellite processing. There the techniques of spectrum shaping at the terminal and/or satellite are considered for controlling inter-user inteference and for coexisting with line-of-sight (LOS) users sharing the same system bandwidth. Although the possibility of coding is also mentioned in the other report, only coherent hard-decision receivers employing no coding are treated here.

The organization of this report is as follows. In the remainder of this section the principal modulation schemes of interest and their associated crosstalk formulas, which are computed later in the report are defined and compared. The subsequent results include estimates of the number of close-packed FDM waveforms that can be accommodated in a 25 kHz or 500 kHz bandwidth by a system tolerant of a 1 dB degradation from one adjacent user. Sections II through V comprise the main body of the report where the detailed crosstalk formulas are derived. Most of the analysis is contained in Section II which treats a fundamental modulation scheme. Sections III through V deal with similar analyses specialized to other forms of modulation. Finally, Section VI discusses a

technical point of interest arising from the derived crosstalk formulas and suggests some directions for future work including M-ary PSK for M > 4.

1.2 Definitions

In this report the following simple model is analyzed for several classes of modulation. Just two mutually interfering waveforms from the same modulation class are considered for mathematical tractability. The receiver consists of a perfect detector for one of these waveforms, called the signal waveform or the waveform being demodulated, that is optimal in the presence of additive white Gaussian noise (AWGN) only. Correct symbol timing, frequency and phase references are assumed for the signal waveform, i.e., the receiver is coherent. The other waveform is called the interfering waveform.

The receiver for each modulation class* is configured to make binary decisions only, and in such a way that the bit error probability P_b for the signal waveform in AWGN only is identical to

$$P_b = \frac{1}{2}\,\mathrm{erfc}\,(\sqrt{E_b/N_o}) = \frac{1}{\sqrt{2\pi}} \int_{\sqrt{\frac{2E_b}{N_o}}}^{\infty} e^{-z^2/2}\,dz \qquad (1.1)$$

corresponding to binary antipodal elementary signals, where E_b is the received signal energy per bit and $N_o/2$ is the double-sided noise density [3]. Equation (1.1) is shown graphically in Fig. 1.1.

Crosstalk is defined as that part of the input to a decision device attributable to the presence of the interfering waveform. The crosstalk can

* Except the M-ary PSK (M > 4) of Section VI and the Appendix.

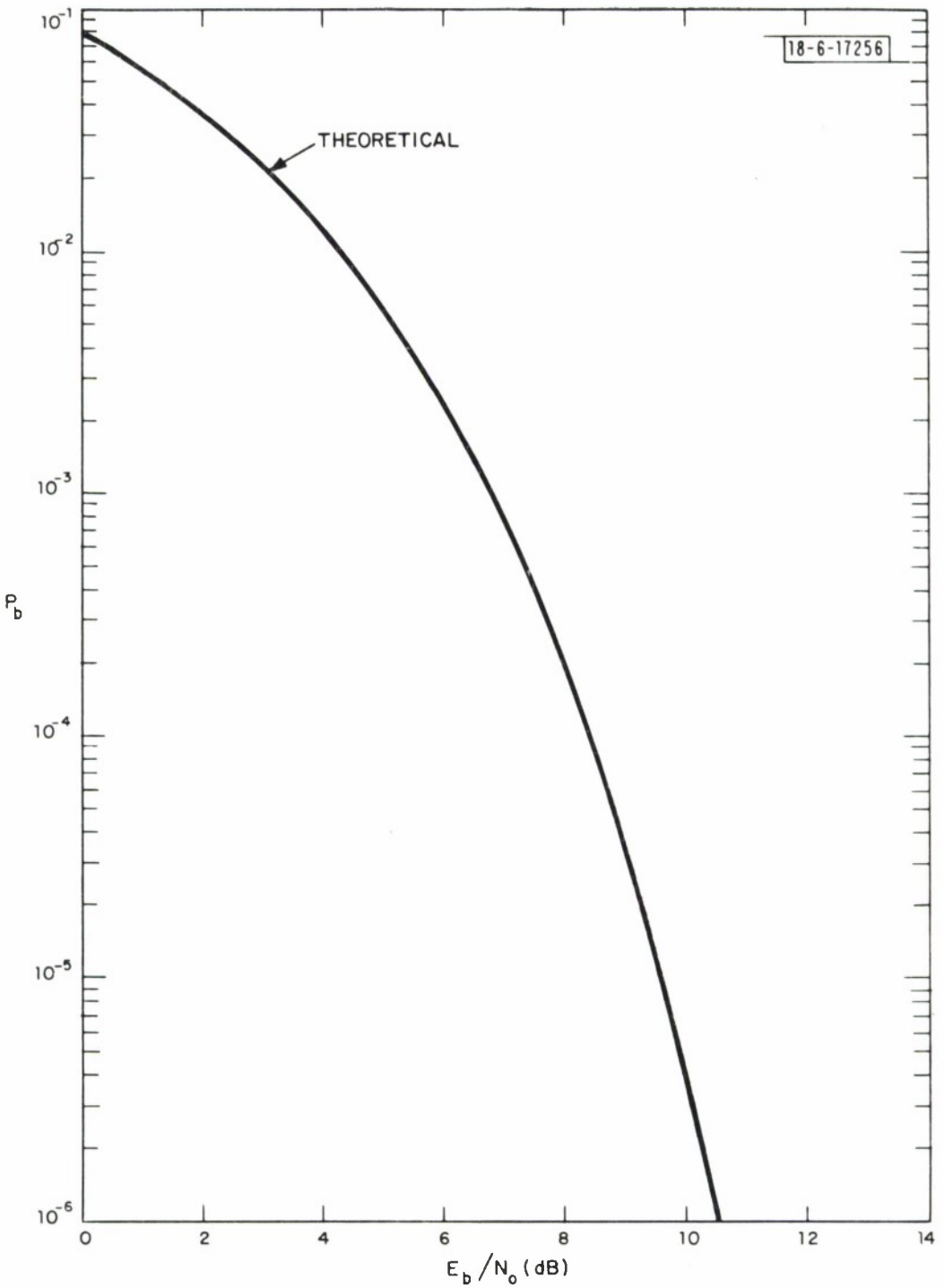

Fig. 1.1. Coherent receiver performance for binary antipodal signals in AWGN.

enhance or degrade the detectability of the signal waveform by increasing or decreasing, respectively, the average effective received signal energy per bit

$$(E_b)_{eff} :=^{*} E_b/L \tag{1.2}$$

where L represents the loss factor due to crosstalk. The resulting bit error probability is usually obtained simply by replacing the E_b of Eq. (1.1) by the $(E_b)_{eff}$ of Eq. (1.2).

The maximum signal energy loss resulting from the most unfortunate circumstances, i.e., the worst-case crosstalk, is of primary concern for obtaining a simple upper bound to P_b. Parenthetically, if C_{max} is the worst-case crosstalk and if λ is a parameter between -1 and +1 specifying a crosstalk level λC_{max}, then the probability $P(\lambda)$ with which the average signal energy is reduced by more than a factor of $L(\lambda)$ is also of interest for obtaining a more refined upper bound as well as a lower bound to P_b. That is, if $P_b(\lambda)$ denotes the bit error probability given λ, and if λ_o is a particular value of λ specifying a certain loss level, then one can bound the bit error probability P_b as

$$P(\lambda_o)\ P_b(\lambda_o) \leq P_b \leq (1-P(\lambda_o))\ P_b(\lambda_o) + P(\lambda_o)\ P_b(1) \leq P_b(1) \tag{1.3}$$

using the fact that $P_b(\lambda)$ is monotone increasing with an increasing threshold level λ. Normally, one would require $P_b(\lambda_o) \lesssim P_b$.

---

* := defines symbol on the left-hand side

Generally, there is quite a gap between these upper and lower bounds. Naturally, it is safer to use an upper bound as an estimate of P_b in a system design. However, because of the rather steep slope of the curve in Fig. 1.1 at lower error rates, one expects the bit error probability to be dominated by values of λ close to unity. One is therefore tempted to write

$$P(\lambda_o)\ P_b(\lambda_o) \leq P_b \overset{\sim}{<} P(\lambda_o)\ P_b(1) \tag{1.4}$$

by ignoring λ's less than some $\lambda_o \overset{\sim}{<} 1$. But a comparison of the right-hand sides of Eqs. (1.3) and (1.4) reveals that the approximate upper bound of Eq. (1.4) could be much too optimistic. In particular, as $\lambda_o \to 1$, $P_b(\lambda_o) \to P_b(1)$ and $P(\lambda_o) \to 0$, and the tighter upper bound of Eq. (1.3) can be approximated by $P_b(\lambda_o)$, provided $P_b(\lambda_o) >> P(\lambda_o)\ P_b(1)$. Under these circumstances the ratio of the upper bound to the lower bound in Eq. (1.3) is approximately $1/P(\lambda_o)$ which is quite a gap for very small $P(\lambda_o)$, while the bounds of Eq. (1.4) would be relatively tight. Thus, caution should be used in applying Eq. (1.4).

An attempt will be made to estimate $P(\lambda)$ for most of the modems considered. Better judgement regarding the bounds of Eq. (1.4) can be rendered with some realistic values for $P(\lambda)$ and $P_b(\lambda)$.

Continuing with some definitions, the information rate R in bits per second (bps) is the same for all modulation schemes. The duration T in sec is defined as $T := 1/R$. The assumed asynchronism between the two waveforms is

characterized by an arbitrary relative delay τ in the symbol timing reference of one waveform in the pair.

The center frequency separation between the two waveforms adjacent in frequency is expressed in terms of the data rate as kR/4 in cycles per second (Hz), where k is an integer* larger than unity. Depending on the modulation, only certain values of the parameter k are permissible. These restrictions on k and the center frequency spacing arise from a generalized orthogonality constraint that guarantees no crosstalk interference between two synchronized waveforms, i.e., two waveforms with a relative delay of $\tau = 0$ (e.g., see Eq. (2.3)).

Throughout the analysis an arbitrary relative amplitude A and phase θ for the interfering waveform with respect to the signal waveform being demodulated is assumed. Absolute phase is irrelevant in all the detection methods used.

The crosstalk formulas and probability $P(\lambda)$ are computed assuming equally likely bit transmissions.

The signal-to-noise ratio (SNR) loss factor $L(\lambda)$ for a given modem can be expressed in terms of a crosstalk formula $S_k(A,\lambda)$ which depends on the relative amplitude A of the interfering waveform and the threshold level λ (see Eq. (2.17)). The parameter k specifies the center frequency separation. The maximum crosstalk value $C_{max} = S_k(A,1)$ occurs if the threshold λ is at its maximum value of unity.

There is no attempt to treat relative Doppler or other frequency uncertainty for the interfering waveform in this report. Although frequency errors up to $\lesssim$ 1 kHz are possible with high-speed aircraft at UHF, this would not

* This is for analytical convenience only and should not be construed as an operational restriction on the center frequency separation (see Section VI).

seriously affect the crosstalk between waveforms supporting data rates of at least 2400 bps for center frequency spacings of interest, e.g., at least 6 kHz. On the other hand, 75 bps waveforms should be separated in frequency by several kHz to withstand such frequency uncertainties.

Next the antipodal modulation schemes examined in this report are defined. Binary phase shift keying (BPSK) is the well-known modulation of a sinusoidal carrier by a rectangular wave assuming values of ±1. Referring to Fig. 1.2, quadriphase shift keying (QPSK) is just the sum of two BPSK modulation channels at the same carrier frequency but in phase quadrature. The bit timing tics are aligned on these channels. Offset or staggered QPSK (SQPSK) is identical to QPSK except that the bit timing reference of one channel is delayed by T [4]. Continuous-phase binary frequency shift keying with the signaling frequency separation* $\Delta f = 1/2T$ (minimum shift keying, or MSK) is the same as SQPSK except that each modulating wave consists of a concatenation of half-cycle sinusoids of duration 2T instead of rectangles [5]. Alternating QPSK (AQPSK) is identical to SQPSK except that the modulating wave for one of the quadrature channels is zero for alternate intervals of duration T, while the modulation for the other channel is zero during the intervening intervals [6,7]. Continuous-phase quadrifrequency shift keying with $\Delta f = 1/4T$ (CPQFSK) is like MSK except that there are four signaling frequencies instead of only two [8,9]. Finally, biorthogonal FSK with $\Delta f = 1/2T$ or $1/4T$ is a 4-ary system where each signaling element is determined by a choice of two frequencies and two signs.

---

* MSK should not be viewed as a form of FSK in this report but as a form of QPSK (see Section 3.4).

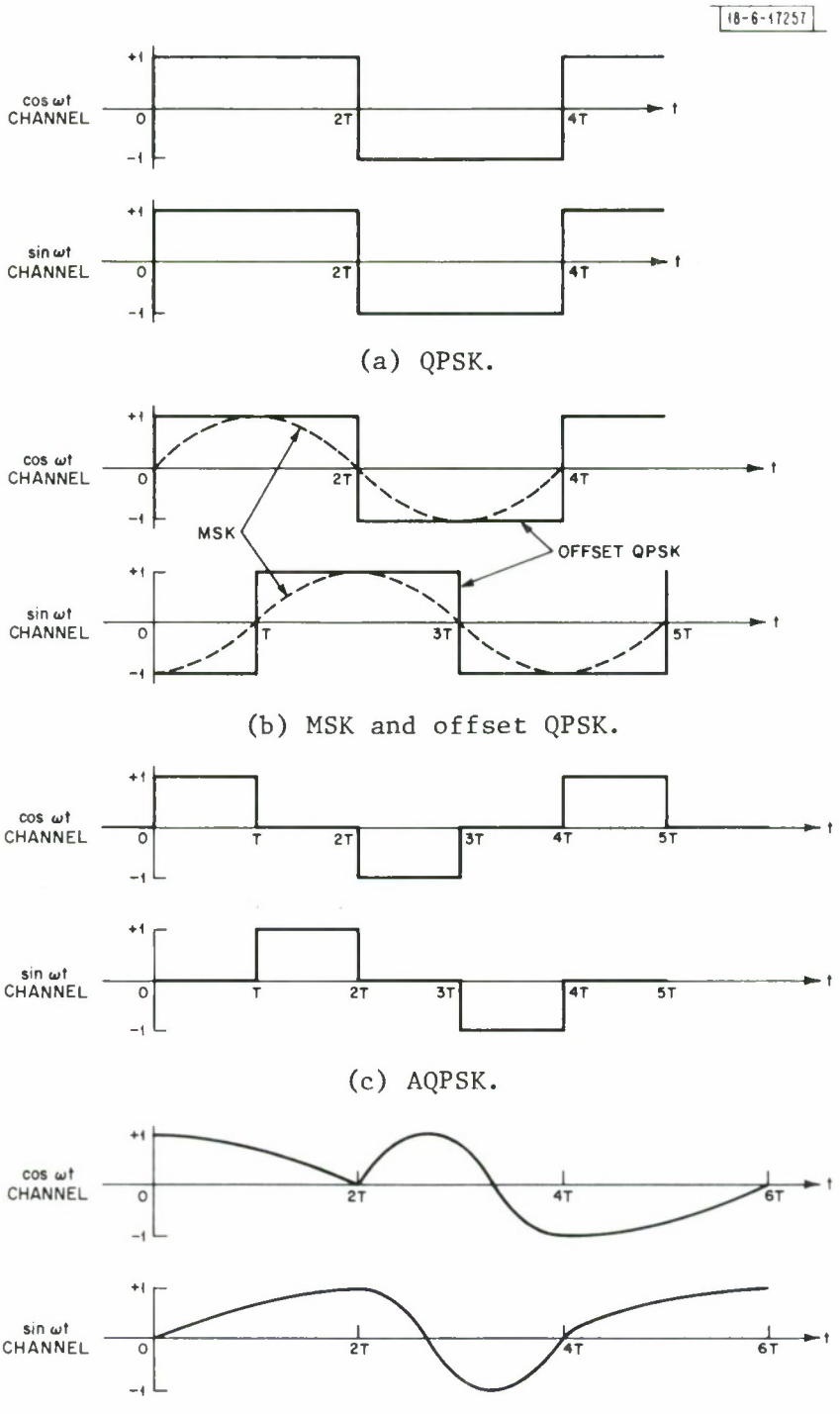

(a) QPSK.

(b) MSK and offset QPSK.

(c) AQPSK.

(d) CPQFSK.

Fig. 1.2. Modulation waveforms.

1.3 Results

In this section the results of the crosstalk analysis are summarized and the various modems are compared from a systems point of view.

The worst-case crosstalk formulas, i.e., those corresponding to the maximum SNR loss, derived in the main body of the report are listed in Table 1.1. The MSK formula for k/2 odd and the CPQFSK results are only approximations. In addition, the worst-case results for CPQFSK were not computed beyond k = 13.

Using Eq. (1.7) and Table 1.1 the worst-case SNR losses for center frequency separations of R, 2R and 3R (k = 4, 8, 12, respectively) are shown in Fig. 1.3. It is observed that continuous-phase FSK generally does far better than the other modulation schemes. In particular, MSK yields much lower losses for a fixed interference level or can withstand much larger interference levels for a fixed SNR loss.

SQPSK, QPSK and AQPSK are 3 dB better than BPSK with respect to the interference level for a fixed SNR loss. However, for equal strength waveforms (A = 1) MSK results in 3.1 dB, 1.9 dB and 1.2 dB less loss than SQPSK, QPSK and AQPSK for separations of R, 2R and 3R, respectively. This advantage becomes much more pronounced at higher levels of interference (A > 1). For example, for a 10 dB interference level (A^2 = 10) this loss advantage of MSK grows to 9.6 dB and 5.1 dB for spacings of 2R and 3R, respectively.

MSK is uniformly superior to CPQFSK and is nearly 6 dB better asymptotically with respect to the interference level for large center frequency spacings. Nevertheless, CPQFSK still outperforms SQPSK, QPSK and AQPSK for the 2R and 3R spacings. Except for the closest spacing R, CPQFSK does considerably better than either of the biorthogonal schemes.

TABLE 1.1

WORST-CASE CROSSTALK FORMULAS

Modulation	$C_{max} = S_k(A,1)$ (see Section 2.2)	
8PSK	$\frac{8A}{\pi k}$,	$k = 4, 8, 12, \ldots$
QPSK	$\frac{4\sqrt{2}A}{\pi k}$,	$k = 2, 4, 6, \ldots$
SQPSK, AQPSK	$\frac{4\sqrt{2}A}{\pi k}$,	$k = 4, 8, 12, \ldots$
MSK	$\frac{8A}{\pi(k^2-4)}$,	$k = 4, 8, 12, \ldots$
	$\frac{8(k+1)A}{\pi k(k^2-4)}$,	$k = 6, 10, 14, \ldots$
biorthogonal FSK (minimal spacing)	$\frac{2(2k-1)A}{\pi k(k-1)}$,	$k = 2, 4, 6, \ldots$
	$\frac{4A}{\pi(k-1)}$,	$k = 3, 5, 7, \ldots$
biorthogonal FSK (double spacing)	$\frac{4A}{\pi(k-2)}$,	$k = 4, 6, 8, \ldots$
	$\frac{4(k-1)A}{\pi k(k-2)}$,	$k = 5, 7, 9, \ldots$
CPQFSK *	$\frac{1.653A}{\pi}$,	$k = 4$
	$\frac{0.8831A}{\pi}$,	$k = 5$
	$\frac{0.5406A}{\pi}$,	$k = 6$
	$\frac{0.3345A}{\pi}$,	$k = 7$
	$\frac{0.2361A}{\pi}$,	$k = 8$
	$\frac{0.1912A}{\pi}$,	$k = 9$
	$\frac{0.1573A}{\pi}$,	$k = 10$
	$\frac{0.1236A}{\pi}$,	$k = 11$
	$\frac{0.1043A}{\pi}$,	$k = 12$
	$\frac{0.0840A}{\pi}$,	$k = 13$

* An exact formula for arbitrary k could not be obtained (see Section 4.2).

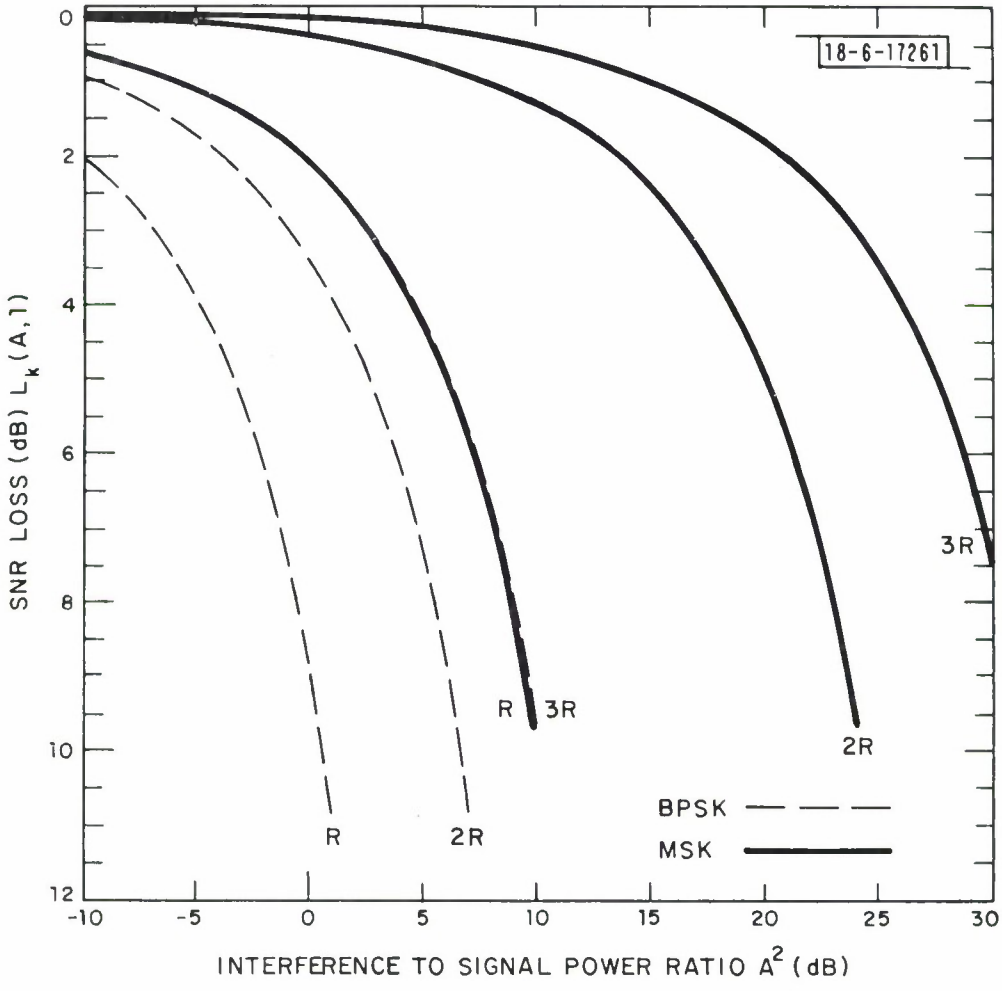

(a) BPSK vs MSK.

Fig. 1.3. Worst-case SNR loss from crosstalk for center frequency separations of R, 2R and 3R.

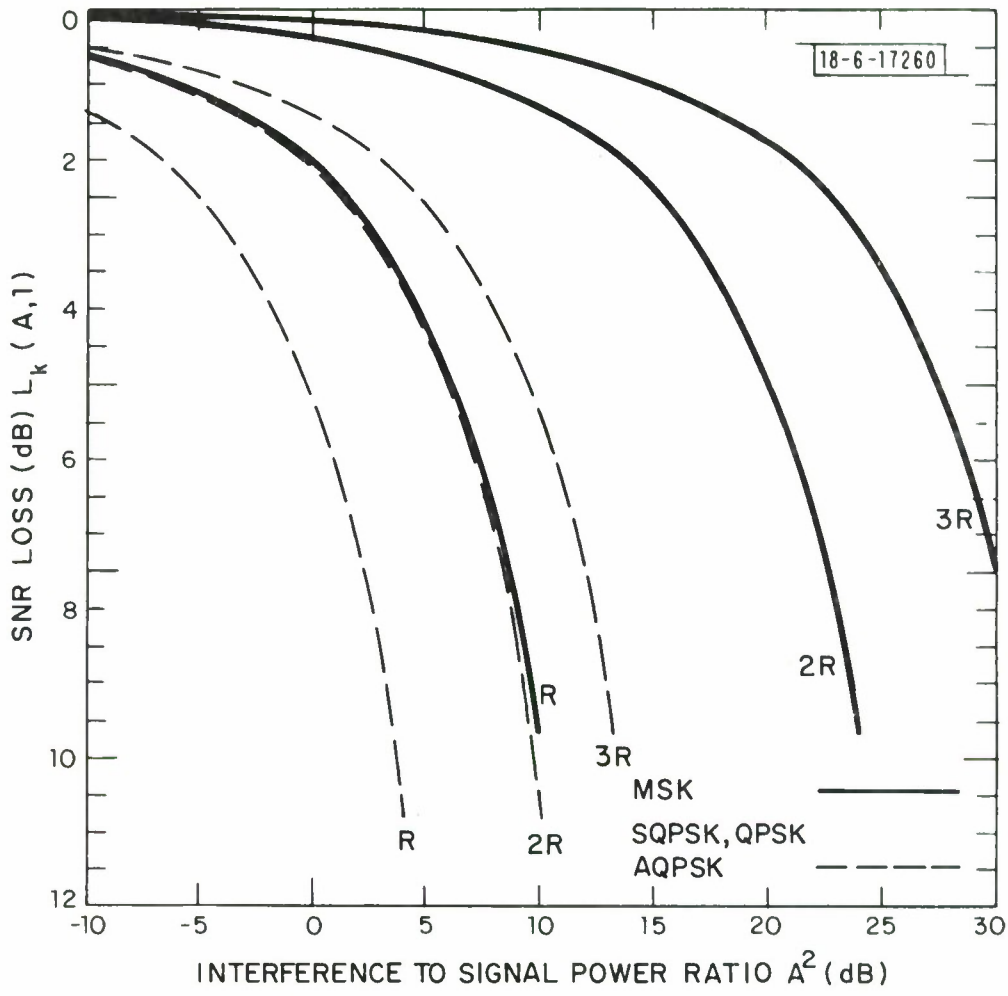

(b) SQPSK, QPSK, AQPSK vs MSK.

Fig. 1.3. Continued.

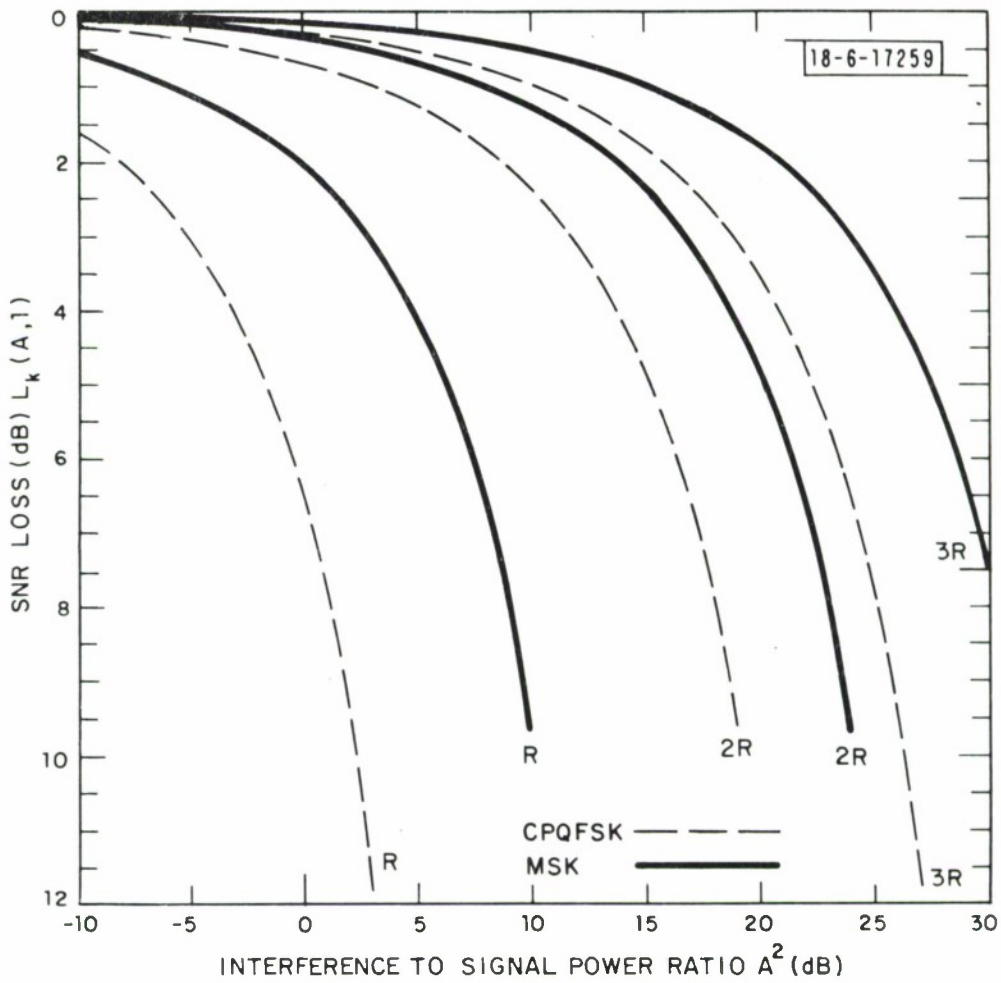

(c) CPQFSK vs MSK.

Fig. 1.3. Continued.

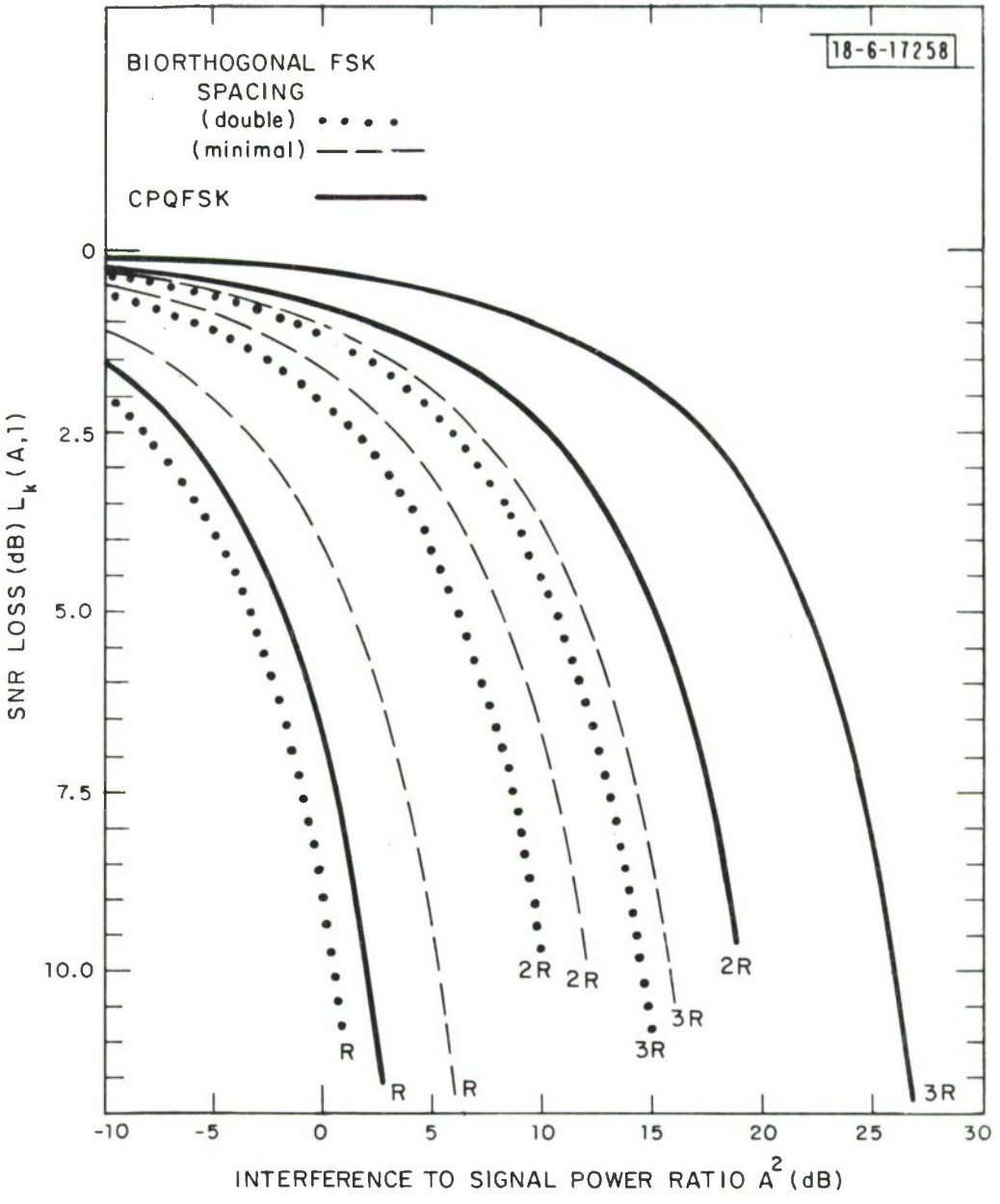

(d) Biorthogonal FSK vs CPQFSK.

Fig. 1.3. Continued.

Note that even the biorthogonal schemes are slightly better than SQPSK, QPSK and AQPSK except for the R center frequency separation and the biorthogonal FSK with the double signaling frequency spacing. Asymptotically, the biorthogonal schemes are 3 dB better.

The superiority of continuous-phase FSK arises from the fact that the power spectrum decreases asymptotically as the inverse square of frequency since the waveforms are continuous. Being discontinuous the waveforms of the other modulation schemes have spectra that decrease as only the inverse of frequency asymptotically. Hence, the MSK and CPQFSK crosstalk formulas can be written as $O(k^{-2})$, while the other formulas are described by $O(k^{-1})$.

In comparison with the other forms of modulation, MSK has the greatest potential for close packing many FDM waveforms in a given bandwidth. This issue will be examined next for both a 0% and a 1% exceedance probability $P(\lambda)$ and a SNR loss of 1 dB or less for several interfering waveform power levels.

The minimal center frequency spacings for the worst-case crosstalks are given in Table 1.2. The spacings for a given modulation scheme were calculated using the permissible values of k for that form of modulation*. The 1 dB SNR loss tolerance is for just one interfering waveform at a received power level A^2 dB above the signal waveform and at an adjacent center frequency. For equal strength users (A = 1)MSK has a close packing bandwidth advantage factor of 4, 10/3, 3, 7/6, and 13/6 compared to BPSK, SQPSK and AQPSK, QPSK, CPQFSK and biorthogonal FSK, respectively. This advantage increases with the interference level. For example, with a 10 dB interference level (A^2 = 10) MSK would consume less than 1/5 the bandwidth necessary for SQPSK, AQPSK or QPSK.

* See Section VI for a discussion of unrestricted center frequency spacings.

TABLE 1.2

MINIMAL PERMISSIBLE CENTER FREQUENCY SEPARATION (Hz) FOR WORST-CASE CROSSTALK (P(1) = 0) AND A SNR LOSS OF 1 dB OR LESS FROM WAVEFORM ADJACENT IN FREQUENCY

	Interference Level A^2(dB)			
Modulation	0	10	20	30
BPSK	6R	19R	59R	186R
SQPSK, AQPSK	5R	14R	42R	131R
QPSK	4.5R	13.5R	41.5R	131R
MSK	1.5R	2.5R	4R	7R
CPQFSK	1.75R	3R	5R*	8.75R*
BIORTHOGONAL FSK				
minimal spacing	3.25R	9.5R	29.5R	93R
double spacing	3.25R	9.75R	29.75R	93.25R

R is the information rate in bits/sec

* estimated.

TABLE 1.3

MINIMAL PERMISSIBLE CENTER FREQUENCY SEPARATION (Hz) FOR 1% CROSSTALK LEVEL ($P(\lambda_o) = 0.01$) AND A SNR LOSS OF 1 dB OR LESS FROM WAVEFORM ADJACENT IN FREQUENCY

	Interference Level A^2(dB)			
Modulation	0	10	20	30
BPSK	6R	18R	56R	175R
SQPSK	4R	12R	37R	116R
QPSK	4R	12R	36.5R	115.5R
AQPSK	5R	13R	41R	127R
MSK	1.5R	2.5R	4R	6.5R
CPQFSK	1.5R	2.5R	4.25R*	7.25R*

R is the information rate in bits/sec

* estimated.

In this worst case the 1 dB SNR loss would be translated into an increase in the probability of bit error simply by moving 1 dB to the left on the curve of Fig. 1.1. By Eq. (1.3) this yields an upper bound to P_b. Thus, to meet a $P_b \leq 10^{-2}$, 10^{-3}, 10^{-4}, or 10^{-5} requirement, an $E_b/N_o \geq$ 5.3 dB, 7.8 dB, 9.4 dB, or 10.6 dB is necessary, respectively.

The spacings for a 1% crosstalk level and all the modulation schemes except biorthogonal FSK are shown in Table 1.3. Comparison with Table 1.2 reveals that somewhat closer spacings are possible. In particular, note that CPQFSK now does as well as MSK for the 0 dB and 10 dB interference levels. At these levels the bandwidth advantage of continuous-phase FSK and SQPSK and QPSK is reduced slightly to a factor of 8/3 and 24/5, respectively. This is because of the negligible bandwidth reduction of MSK and the 10% to 20% bandwidth savings for SQPSK, QPSK and CPQFSK for the 1% crosstalk level.

The λ_o's that yielded $P(\lambda_o) = 0.01$ are listed in Table 1.4. Recall that the crosstalk exceeds $\lambda_o C_{max}$ 1% of the time, where C_{max} is the worst-case crosstalk. From Eq. (1.3) P_b can be upper bounded by $0.99\ P_b(\lambda_o) + 0.01\ P_b(1)$. Calculations using Tables 1.1, 1.3 and 1.4 show that the difference in SNR loss for the 1% crosstalk level compared with the worst case is no more than a few tenths of a dB. Therefore this refined bound of Eq. (1.3) is not significantly different than the worst-case bound $P_b(1)$. This can be seen from the small difference $P_b(1) - P_b(\lambda_o)$ implied by a few tenths of a dB change in E_b/N_o in Fig. 1.1.

Thus, although the SNR losses are indeed reduced slightly for the 1% crosstalk tolerance, the implied bandwidth reductions of Table 1.3 over

TABLE 1.4

THRESHOLD VALUE λ_o FOR $P(\lambda_o) = 0.01$ DEFINING 1% CROSSTALK LEVEL

	Interference Level A^2(dB)			
Modulation	0	10	20	30
BPSK	←	0.94	→	
SQPSK, QPSK	←	0.88	→	
AQPSK	←	0.97	→	
MSK	0.77	0.79	0.88*	0.87*
CPQFSK	0.6	0.68*	0.68*	0.68*

* estimated.

TABLE 1.5

MAXIMUM NUMBER OF UNSYNCHRONIZED R = 2400 bps WAVEFORMS IN 25 kHz BANDWIDTH ($\leq$ 1 dB SNR LOSS FROM WAVEFORM ADJACENT IN FREQUENCY)

	Interference Level A^2(dB)			
Modulation	0	10	20	30
BPSK	2	1	1	1
SQPSK, QPSK, AQPSK	3	1	1	1
MSK	7	5	3	2
CPQFSK				
$P(1) = 0$	6	4	3	2
$P(\lambda_o) = 0.01$	7	5	3	2
BIORTHOGONAL FSK				
$P(1) = 0$	4	2	1	1

Table 1.2 for the worst-case tolerance are more significant. The refined (1%) threshold analysis would have a greater effect on the SNR losses if the minimal center frequency spacings were based on a SNR loss larger than 1 dB. That is, with greater crosstalk from an interfering waveform adjacent in frequency, the SNR loss difference is more sensitive to changes in the crosstalk threshold level λ. On the other hand, the bandwidth savings accrued from lowering the threshold λ at a fixed SNR loss are essentially independent of the loss level. This can be verified by studying the crosstalk formulas of Table 1.1.

Using Tables 1.2 and 1.3 the maximum number of uncoordinated waveforms that can be packed into a 25 kHz and 500 kHz bandwidth are listed in Tables 1.5 and 1.6, respectively. The entries were computed as the least integer no less than the bandwidth divided by the minimum center frequency spacing for $\stackrel{<}{-}$ 1 dB SNR loss from an adjacent waveform. For the 25 kHz bandwidth and 2400 bps waveforms of Table 1.5, the threshold analysis increased the number of waveforms only for CPQFSK and the 0 dB and 10 dB interference levels. For the 500 kHz bandwidth and 2400 bps and 16 kbps waveforms of Table 1.6 the effect of the threshold analysis is more pronounced. The increase in the number of waveforms with the 1% tolerance is larger for SQPSK, QPSK and CPQFSK. Note that MSK and CPQFSK yield nearly the same numbers in Table 1.6b.

1.4 Conclusions

The crosstalk properties of nominally identical but uncoordinated FDM waveforms processed by optimal coherent receivers over an AWGN channel have been studied in this report. No power control or interwaveform timing or

TABLE 1.6

MAXIMUM NUMBER OF UNSYNCHRONIZED WAVEFORMS IN 500 kHz BANDWIDTH ($\leq$ 1 dB SNR LOSS FROM WAVEFORM ADJACENT IN FREQUENCY)

a. Worst-Case Center Frequency Spacings P(1) = 0

Modulation	Information Rate R(bps) 2400 Interference Level A^2(dB)				16000 Interference Level A^2(dB)			
	0	10	20	30	0	10	20	30
BPSK	35	11	4	1	6	2	1	1
SQPSK, AQPSK	42	15	5	2	7	3	1	1
QPSK	47	16	6	2	7	3	1	1
MSK	139	84	53	31	21	13	8	5
CPQFSK	119	70	42	24	18	11	7	4
BIORTHOGONAL FSK	65	22	8	3	10	4	2	1

b. 1% Tolerance Threshold ($P(\lambda_o) = 0.01$)

Modulation	Information Rate R(bps) 2400 Interference Level A^2(dB)				16000 Interference Level A^2(dB)			
	0	10	20	30	0	10	20	30
BPSK	35	12	4	2	6	2	1	1
AQPSK	42	17	6	2	7	3	1	1
SQPSK, QPSK	53	18	6	2	8	3	1	1
MSK	139	84	53	33	21	13	8	5
CPQFSK	139	84	50	29	21	13	8	5

Doppler requirements were imposed on the transmitters. Each receiver was assumed to acquire and track the signal waveform. Crosstalk was combatted merely by sufficient center frequency spacing between the waveforms. No other special processing was applied. The following related conclusions have been established.

A. CONTINUOUS-PHASE FSK MODULATION REQUIRES MUCH LESS SYSTEM BANDWIDTH THAN BIORTHOGONAL FSK AND THE VARIOUS FORMS OF PSK MODULATION

Even with perfect power control at the transmitters (A = 1), CPFSK requires only one third the bandwidth necessary for SQPSK, AQPSK or QPSK. The bandwidth advantage of CPFSK increases to a factor of 5 or 10 when the interference power level is permitted to vary by as much as 10 dB ($A^2 = 10$) or 20 dB ($A^2 = 100$), respectively. The advantage of CPFSK over BPSK is even greater than for the quadriphase modulation schemes.

B. CPFSK PERMITS MANY MORE FDM WAVEFORMS IN A GIVEN BANDWIDTH

With perfect power control six or seven 2400 bps CPFSK waveforms can occupy a 25 kHz bandwidth while only two or three such PSK waveforms are possible. For 10 dB interference levels the number of CPFSK waveforms is reduced to four or five but then only one PSK waveform is permitted. In a 500 kHz bandwidth, 139 2400-bps or 21 16-bps CPFSK waveforms are possible with perfect power control. At the 10 dB interference level 84 2400-bps or 13 16-bps waveforms are possible. These are roughly three to five times the number of PSK waveforms possible.

C. CPFSK GREATLY ALLEVIATES THE PROBLEM OF TRANSMITTER POWER CONTROL FOR UNSYNCHRONIZED WAVEFORMS.

The results show that for a fixed level of interference, the SNR loss is much smaller for CPFSK. Alternatively, a much larger interference level can be tolerated for a given SNR loss. See Fig. 1.3.

D. BINARY AND 4-ARY CPFSK ARE ALMOST EQUALLY ATTRACTIVE

For the 1 dB SNR loss level MSK is slightly better than CPQFSK with respect to bandwidth conservation but the differences are significant only for the worst-case crosstalk analysis. CPQFSK requires the generation of four frequencies instead of only two but the symbol timing problem is simpler than with MSK.

E. THE 4-ARY PSK SCHEMES ARE UNIFORMLY BETTER THAN BPSK BUT GENERALLY INFERIOR TO BIORTHOGONAL FSK.

The crosstalk varies as only the inverse of the center frequency separation for all these modulation schemes. With CPFSK the crosstalk varies as the inverse square of the separation.

F. THE ADVANTAGES OF MSK OVER THE OTHER FORMS OF MODULATION ARE SLIGHTLY GREATER FOR THE WORST-CASE CROSSTALK ANALYSIS

The bandwidth requirements for SQPSK, QPSK and CPQFSK are reduced by 10% to 20% when the system is designed to a crosstalk level that is exceeded just 1% of the time. However, the advantages of CPFSK are hardly diminished at such a tolerance level. It is unlikely that a system would be designed with an exceedance probability much larger than $P(\lambda_o) = 0.01$.

G. A REFINED CROSSTALK ANALYSIS REDUCES THE SNR LOSS BY JUST A FRACTION OF A DB

Thus, the worst-case analysis is adequate for establishing performance levels.

H. M-ARY PSK (M > 4) IS INFERIOR TO MSK FOR VALUES OF M AND CENTER FREQUENCY SPACINGS OF INTEREST WITHOUT ADDITIONAL SPECTRAL SHAPING

See Section VI and the Appendix. Special processing for spectral shaping is discussed in the companion report [2].

II. CROSSTALK ANALYSIS FOR OFFSET QPSK (SQPSK)

Of the modulation schemes considered in this report, offset quadriphase shift keying was the candidate selected for the exposition of ideas. The principal reason for this is that once the crosstalk derivation for offset QPSK is understood, the closely related instances of BPSK, QPSK, AQPSK and MSK are more easily handled. The relationship between offset QPSK and biorthogonal FSK or CPQFSK is not quite as direct; the latter two schemes are perhaps more similar to the MSK case.

Although offset QPSK may be in vogue for other reasons, it was not selected for the exposition because of its good crosstalk properties. In fact, continuous-phase FSK modulation results in much less crosstalk then offset QPSK or the other modulation schemes considered, as will be seen. In any event, offset QPSK is treated in this section, followed by BPSK, QPSK, AQPSK and MSK in Section III, CPQFSK in Section IV, and biorthogonal FSK in Section V.*

2.1 Derivation of Crosstalk Formulas

A SQPSK signal at the center frequency ω has the form $\pm \cos \omega t \pm \sin \omega t$, where one of the four possible sign combinations holds for each interval $nT \leq t < (n + 1)T$, $n = 0, \pm 1, \pm 2, \cdots$. As shown in Fig. 2.1 the sign of $\cos \omega t$ is determined by the rectangular modulation waveform assuming the values $a_n = \pm 1$ with transitions at $t = 2nT$. The sign of $\sin \omega t$ is determined by the rectangular waveform assuming the values $b_n = \pm 1$ with transitions at $t = (2n - 1)T$. An optimal receiver for this SQPSK signal in AWGN is shown in Fig. 2.2; $\hat{a}_n$ and

---

* M-ary PSK is treated separately in Section VI and the Appendix because antipodal signaling is not possible for $M > 4$ with M-ary PSK.

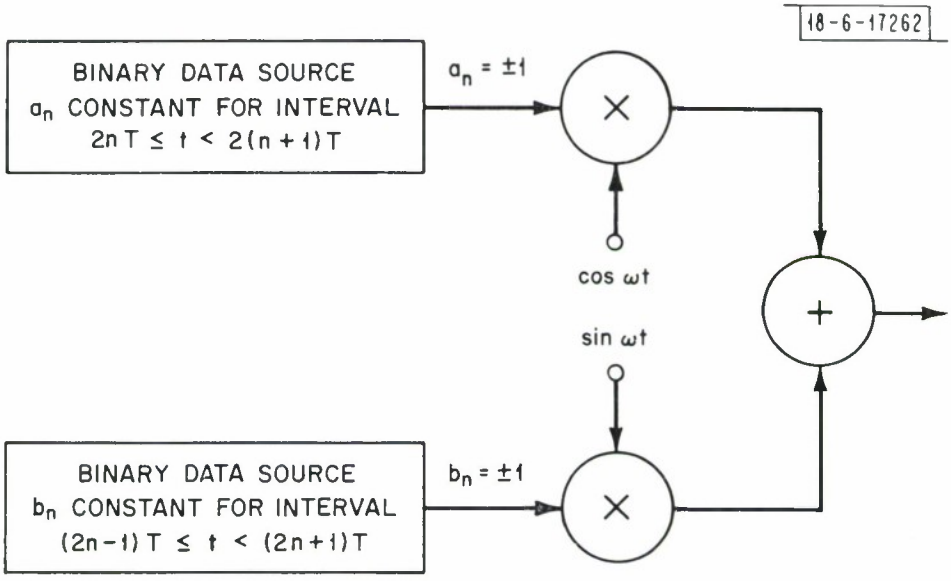

Fig. 2.1. Offset QPSK transmitter.

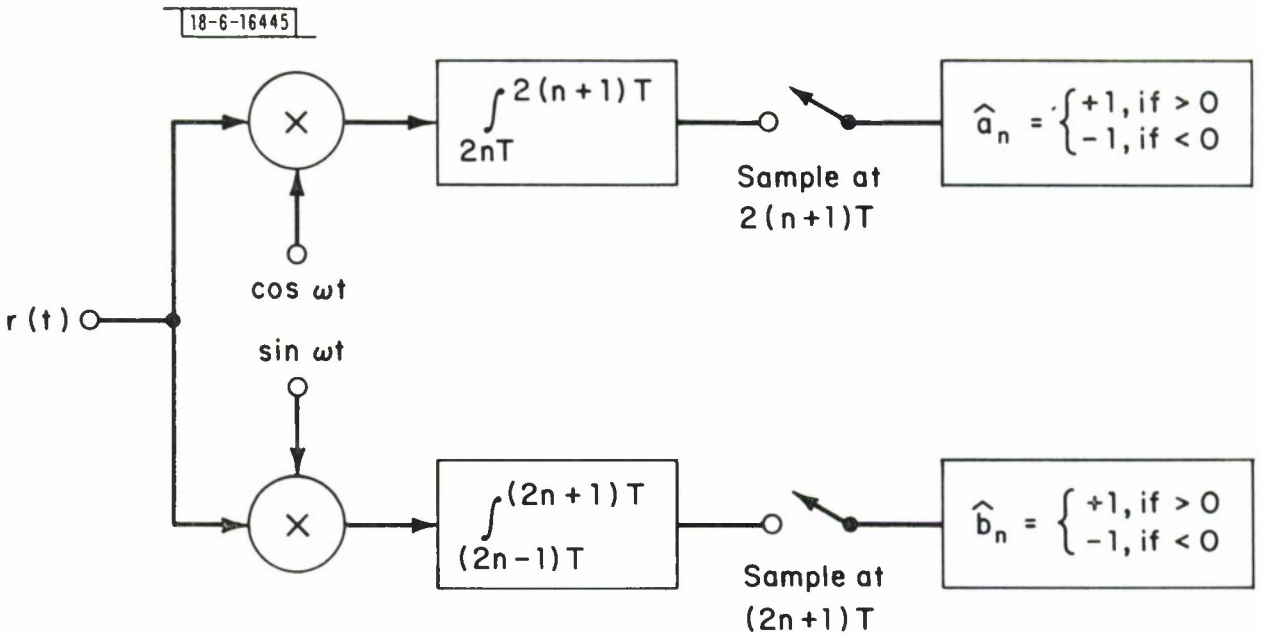

Fig. 2.2. Offset QPSK receiver.

$\hat{b}_n$ are estimates of a_n and b_n, respectively. For the purpose of crosstalk analysis the channel noise is ignored. Thus, the received waveform from two SQPSK users has the form

$$r(t) = \pm \cos \omega t \pm \sin \omega t \pm A \cos (\nu(t - \tau) + \theta) \pm A \sin (\nu(t - \tau) + \theta) \quad (2.1)$$

where the amplitude signs are mutually independent. The interfering waveform of magnitude A and center frequency $\nu \neq \omega$ is delayed by $0 \leq \tau < 2T$ with respect to the waveform of unit magnitude that is to be demodulated. An arbitrary phase θ for the interfering waveform is also included in the model.

Without loss of generality only the upper demodulation channel of Fig. 2.2 for n = 0 and a delay of $0 \leq \tau \leq T$ in Eq. (2.1) need be considered. The $T < \tau < 2T$ situation is equivalent to advancing the interfering waveform by $0 < 2T - \tau < T$ with the modulating data sequences for the other waveform advanced by 2T. An advance of $0 < \tau' < T$ for the interfering waveform is equivalent to changing the sign of τ and θ throughout the crosstalk formulas and modifying the modulating data. However, the particular data sequences involved are irrelevant for statistically independent and equally likely bits in each sequence.

Several trigonometric identities are used implicitly in the following crosstalk derivations. All sum frequency terms are ignored since their contribution after integration is negligible compared to the difference frequency terms, assuming that $\omega, \nu >> \omega - \nu$. For notational convenience, let

$$\Delta := \omega - \nu \qquad v := \nu\tau - \theta \qquad w := \omega\tau - \theta = v + \Delta\tau \quad . \quad (2.2)$$

By demanding that there be no crosstalk for synchronized* users, i.e., no SNR loss in the detectability of a_0 for $\tau = 0$ due to the interfering waveform, the center frequency constraint

$$\Delta T = 2\pi k', \quad k' = 1, 2, 3, \ldots \tag{2.3}$$

will be justified, cf. Cases 1 and 3 below.

Performing the cos ωt multiplication of Fig. 2.2 on Eq. (2.1) the input to the upper integrator becomes

$$\frac{1}{2} (\pm 1 \pm A \cos(\Delta t + v) \mp A \sin(\Delta t + v). \tag{2.4}$$

The constant term constituting the signal integrates to $a_0 T$. The remaining terms representing the interference will be integrated for the following four possible changes of sign in the data sequences of the interfering waveform:

Case 0: no change at τ and no change at $T + \tau$

$$\frac{A}{2} \int_0^{2T} \Big(\pm \cos(\Delta t + v) \mp \sin(\Delta t + v)\Big) dt$$

$$= \frac{A}{2\Delta} \Big(\pm(\sin(2\Delta T + v) - \sin v) \pm (\cos(2\Delta T + v) - \cos v)\Big)$$

$$= 0, \text{ by Eq. (2.3)} \quad .$$

---

* In this model the relative Doppler or other frequency uncertainty is assumed to be zero.

Case 1: no change at τ and change at $T + \tau$

$$\frac{A}{2}\left(\pm\int_0^{2T}\cos(\Delta t + v)dt \mp\left(\int_0^{T+\tau}\sin(\Delta t + v)dt - \int_{T+\tau}^{2T}\sin(\Delta t + v)dt\right)\right)$$

$$= \pm\frac{A}{\Delta}\left(\cos(\Delta T + v + \Delta\tau) - \cos v\right)$$

$$= \pm\frac{A}{\Delta}\left(\cos w - \cos v\right), \text{ by Eqs. (2.2) and (2.3)} \quad .$$

One would have crosstalk for $\tau = 0$ if $\Delta T \not\equiv 0 \pmod{2\pi}$, hence, Eq. (2.3) is justified.

Case 2: change at τ and no change at $T + \tau$

$$\frac{A}{2}\left(\pm\left(\int_0^{\tau}\cos(\Delta t + v)dt - \int_{\tau}^{2T}\cos(\Delta t + v)dt\right) \mp\int_0^{2T}\sin(\Delta t + v)dt\right)$$

$$= \pm\frac{A}{\Delta}\left(\sin w - \sin v\right), \text{ by Eqs. (2.2) and (2.3)} \quad .$$

Case 3: change at τ and change at $T + \tau$

$$\frac{A}{2}\left(\pm\left(\int_0^{\tau}\cos(\Delta t + v)dt - \int_{\tau}^{2T}\cos(\Delta t + v)dt\right)\right.$$
$$\left.\mp\left(\int_0^{T+\tau}\sin(\Delta t + v)dt - \int_{T+\tau}^{2T}\sin(\Delta t + v)dt\right)\right)$$

$$= \frac{A}{\Delta}\left(\pm\left(\sin w - \sin v\right) \pm\left(\cos w - \cos v\right)\right) \quad .$$

This is the sum of the crosstalks for Cases 1 and 2 with independent sign choices. Again, Eq. (2.3) is justified.

Let $C_i(\tau, \theta)$ denote the crosstalk to signal ratio for Case i, i = 0, 1, 2, 3, i.e., the crosstalk expression just derived for Case i divided by a_0T. Recalling Eq. (2.2) and that R = 1/T, one has the normalized crosstalks:

$$C_0(\tau, \theta) = 0 \tag{2.5a}$$

$$C_1(\tau, \theta) = \pm \frac{AR}{\omega-\nu} (\cos(\omega\tau-\theta) - \cos(\nu\tau-\theta)) \tag{2.5b}$$

$$C_2(\tau, \theta) = \pm \frac{AR}{\omega-\nu} (\sin(\omega\tau-\theta) - \sin(\nu\tau-\theta)) \tag{2.5c}$$

$$C_3(\tau, \theta) = C_1(\tau, \theta) + C_2(\tau, \theta) \quad . \tag{2.5d}$$

Regarding A, R, ω and ν as fixed parameters and treating τ and θ as random variables, a probability $P_i(\lambda)$ can be assigned to the event that $C_i(\tau, \theta)$ exceeds a certain threshold level specified by λ. This will quantify the likelihood of a certain SNR degradation due to destructive interference and is the subject of the next section.

2.2 A Threshold Analysis

For simplicity it is assumed that the τ and θ of Eq. (2.5) are uniformly distributed in the ranges $[0, T]$ and $[0, 2\pi]$, respectively, and that every bit of each data sequence is selected independently and with equal probability from $\{+1, -1\}$.

Let the worst-case crosstalk be defined as, cf. Eq. (2.5)

$$C_{max} := \max_{i,\tau,\theta} C_i(\tau, \theta) \quad . \tag{2.6}$$

If C_i denotes the event that Case i occurs, then $Pr(C_i) =: p_i = 1/4$. For λ in the range $[-1, 1]$, the conditional probability distribution $P_i(\lambda)$ is defined as

$$P_i(\lambda) := Pr(C_i(\tau, \theta) > \lambda\, C_{max} \mid C_i) \quad . \tag{2.7}$$

Because of the strict inequality above, note that $P_0(\lambda) = 0$ for $\lambda \geq 0$ and $P_0(\lambda) = 1$ for $\lambda < 0$ for $C_0(\tau, \theta) = 0$. The random data assumption and the sign choices of Eq. (2.5 b,c) imply the symmetry property $P_i(\lambda) + P_i(-\lambda) = P_i(-1) = 1$, $i \neq 0$ or $i = 0$ and $\lambda \neq 0$, which holds for any joint distribution of τ and θ. By plotting $C_1(\tau, \theta)$ on the x axis and $C_2(\tau, \theta)$ on the y axis in the plane, it is not difficult to establish geometrically that

$$P_1\left(\frac{\lambda}{\sqrt{2}}\right) = P_2\left(\frac{\lambda}{\sqrt{2}}\right) = P_3(\lambda)$$

for the crosstalks of Eq. (2.5 b,c,d).

Given that Case i occurs, the probability that the interference is destructive is

$$Pr(C_i(\tau, \theta) > 0 \mid C_i) = P_i(0) \quad . \tag{2.8}$$

For the crosstalks of Eq. (2.5), $P_0(0) = 0$ and $P_i(0) = 1/2$, $i = 1, 2, 3$. The principal function of interest is the overall probability $P(\lambda)$ that the crosstalk exceeds the threshold λC_{max}:

$$P(\lambda) := \sum_i P_i(\lambda) p_i \quad . \tag{2.9}$$

Usually positive values of λ relatively close to unity will be more meaningful in a system design. The summation of Eq. (2.9) simplifies for certain ranges of λ, e.g., $P_0(\lambda) = 0$ for $\lambda \geq 0$ and $P_1(\lambda) = P_2(\lambda) = 0$ for $1/\sqrt{2} \leq \lambda \leq 1$, by Eqs. (2.5) – (2.7).

In addition to $P(\lambda)$, for a given Case i two values of λ are of secondary interest, namely, the peak and mean values of λ attainable with destructive interference. The peak value of λ for Case i is defined as

$$\hat{\lambda}_i := \max_{\tau,\theta} \{\lambda | C_i(\tau,\theta) = \lambda C_{max}\} \quad . \tag{2.10}$$

Of course, $P_i(\lambda_i) = 0$. If $q(\lambda|C_i)$ is the conditional probability density associated with the conditional distribution function $Q_i(\lambda) := 1 - P_i(\lambda)$, then

$$P_i(\lambda) =: \int_\lambda^1 q(z|C_i)\, dz \tag{2.11}$$

and the mean values of λ with destructive interference becomes

$$\begin{aligned} \bar{\lambda}_i &:= E(\lambda | C_i(\tau, \theta) > 0, C_i) \\ &= \frac{\int_0^1 \lambda\, q(\lambda|C_i)\, d\lambda}{P_i(0)} \quad , \; P_i(0) \neq 0 \quad . \end{aligned} \tag{2.12}$$

The average values of these peak and mean parameters are quantitative

indicators of the separation between worst-case and more typical crosstalk interference:

$$E(\hat{\lambda}_i) = \sum_i \hat{\lambda}_i \, p_i \tag{2.13}$$

$$E(\bar{\lambda}_i) = \sum_i \bar{\lambda}_i \, P_i(0) \, p_i \quad . \tag{2.14}$$

For SQPSK, $C_{max} = 2\sqrt{2}\,AR/(\omega - \nu)$, $\hat{\lambda}_0 = 0$, $\hat{\lambda}_1 = \hat{\lambda}_2 = 1/\sqrt{2}$, $\hat{\lambda}_3 = 1$, $\bar{\lambda}_1 = \bar{\lambda}_2 \doteq 0.286$ and $\bar{\lambda}_3 \doteq 0.405$. Thus, since $E(\hat{\lambda}_i) = (1 + \sqrt{2})/4 \doteq 0.6035$ and $E(\bar{\lambda}_i) \doteq 0.122$ there is a significant gap between the worst and more typical cases of interference. Computer generated plots of $P_i(\lambda)$ are shown in Fig. 2.3 with the abscissa scaled by a factor of 1/4, the probability of Case i occurring. Thus, the abscissa gives the actual percentage of time Case i occurs with destructive interference and the crosstalk exceeding $2\sqrt{2}\,AR\lambda/(\omega - \nu)$ for $0 \leq \lambda \leq 1$. The curves for P_1 and P_2 are identical to the P_3 curve except that λ is replaced by $\lambda/\sqrt{2}$. From these curves one obtains $P(0) = 3/8$, $P(1/2) \doteq 0.095$, $P(1/\sqrt{2}) \doteq 0.024$, and of course, $P(1) = 0$. These figures mean that destructive interference occurs 3/8 of the time, that crosstalk is within at least 1/2 of the worst possible value 9.5% of the time and within 3 dB of the worst 2.4% of the time, and that the worst case occurs with probability zero. One could design a system for the SNR loss corresponding to the λ for a 1%, 5% or 10% level of tolerance, say. A formula for SNR loss will be established after defining a frequency spacing parameter k that can be used for all the modulation schemes considered in this report.

Let the center frequency spacing Δf in Hz between the two users be specified by the data rate $R = 1/T$ in bps and the positive integer k defined by

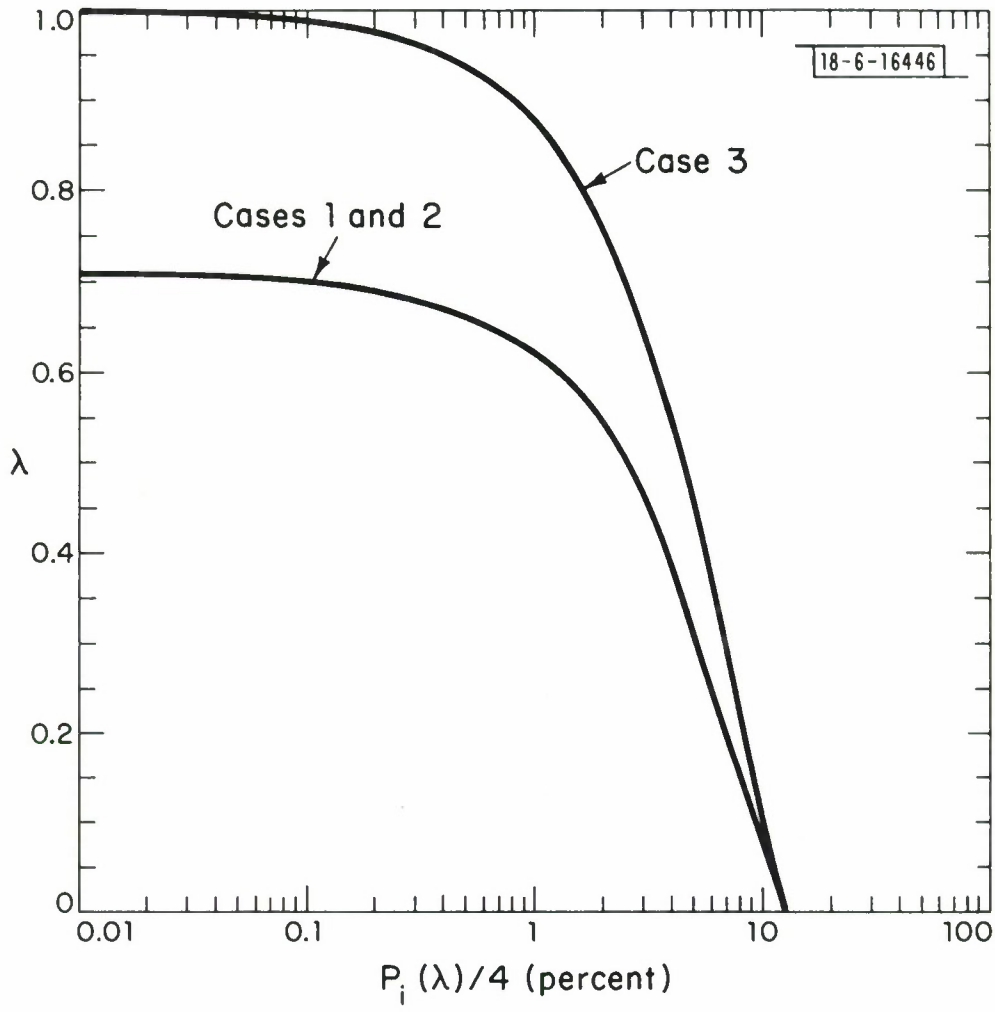

Fig. 2.3. SQPSK crosstalk probabilities.

$$\Delta f =: \frac{kR}{4}, \quad k = 2, 3, 4, \ldots \quad . \tag{2.15}$$

For SQPSK $\Delta f = (\omega - \nu)/2\pi = \Delta/2\pi$, and by the orthogonality condition of Eq. (2.3) the permissible values of k are 4, 8, 12,... . Now for a given k the normalized crosstalk signal can be denoted by $S_k(A, \lambda)$. The crosstalk exceeds $S_k(A, \lambda)$ with probability $P(\lambda)$. For SQPSK,

$$S_k(A, \lambda) = \frac{2\sqrt{2}\, AR\lambda}{\omega - \nu}$$

$$= \frac{4\sqrt{2}\, A\lambda}{\pi k}, \quad k = 4, 8, 12, \ldots \quad . \tag{2.16}$$

If $\lambda > 0$ and $S_k(A, \lambda) \leq 1$, the corresponding SNR loss in dB

$$L_k(A, \lambda) := -20 \log_{10} (1 - S_k(A, \lambda)) \text{ dB}$$

$$\lambda > 0, \quad S_k(A, \lambda) \leq 1 \tag{2.17}$$

is meaningful in the sense that the actual SNR degradation does not exceed $L_k(A, \lambda)$ with probability $1 - P(\lambda)$.

If $S_k(A, \lambda) > 1$, which implies that $\lambda > 0$, the satellite is captured by the interfering signal in the following sense. There is at least one case where the demodulated data bit is determined by the sign of the crosstalk and is independent of the a_0 transmitted by the user being demodulated. For Case i this would imply a bit error probability of at least $P_i(\lambda)$ in the absence of noise. This is a lower bound since there is a decrease in SNR for $0 < \lambda' < \lambda$ which could also result in a decision error. Hence, if $S_k(A, \lambda) > 1$ one can at least lower bound the bit error probably P_b by

$$P_b \geq \sum_i P_i(\lambda)\, p_i, \quad S_k(A, \lambda) > 1 \quad . \tag{2.18}$$

It is remarked that the foregoing crosstalk analysis for SQPSK is essentially unchanged if another arbitrary phase ϕ were added to ωt and νt of Eq. (2.1) and Figs. 2.1 and 2.2 because only difference frequencies are relevant in obtaining Eq. (2.4). Thus, it does not matter at all from the point of view of this crosstalk model whether the a_n data stream modulates cos ωt or sin ωt, for example.

III. CROSSTALK FOR BPSK, QPSK, AQPSK AND MSK

The remainder of this report will sketch the derivations of the crosstalk formulas for other modulation schemes, namely, BPSK, QPSK, AQPSK, MSK, CPQFSK and biorthogonal FSK. Since the bit error probability vs E_b/N_o is the same for these schemes as for SQPSK, the crosstalk performances can be compared on a common basis. The BPSK and QPSK crosstalk formulas can be obtained directly from those already obtained for SQPSK. Although the derivations for MSK are more involved, there are strong similarities between SQPSK and MSK modulation. The major difference is the shape of the modulation waveforms. Thus, it has been advantageous to consider SQPSK first.

3.1 Binary PSK

BPSK modulation is obtained from SQPSK by simply removing the quadrature waveform and halving the signaling interval to keep the same data rate. The received waveform would then have the form, cf. Eq. (2.1)

$$r(t) = \pm \cos \omega t \pm A \cos(\nu(t - \tau) + \theta) \quad . \tag{3.1}$$

Again, the absolute phase of the component waveforms doesn't matter. An optimal AWGN receiver would consist of the upper demodulation channel of Fig. 2.2 except that 2T is replaced by T. BPSK has the same orthogonality constraint as SQPSK, so Eq. (2.3) applies. The Case 0 crosstalk is identically zero, and the Case 1 crosstalk yields the same formula as Case 2 of SQPSK. Since the integration interval is half as long as with SQPSK, the normalized crosstalk formulas for BPSK are

$$C_0(\tau, \theta) = 0 \tag{3.2a}$$

$$C_1(\tau, \theta) = \pm \frac{2AR}{\omega - \nu} (\sin(\omega\tau - \theta) - \sin(\nu\tau - \theta)) \quad . \tag{3.2b}$$

Now $p_i = 1/2$, $C_{max} = 4AR/(\omega - \nu)$, $\hat{\lambda}_0 = 0$, $\hat{\lambda}_1 = 1$, and $\bar{\lambda}_1 \doteq 0.405$. Thus $E(\hat{\lambda}_i) = 1/2$ and $E(\bar{\lambda}_i) \doteq 0.101$, so there is about the same gap between the worst and typical cases of interference compared to SQPSK. The P_1 BPSK curve is identical to the P_3 curve of Fig. 2.2 for SQPSK except that the abscissa is scaled by 1/2 instead of 1/4. Hence, one obtains $P(0) = 1/4$, $P(1/2) \doteq 0.09$ and $P(1/\sqrt{2}) \doteq 0.048$. For BPSK, cf. Eq. (2.16)

$$S_k(A, \lambda) = \frac{8A\lambda}{\pi k}, \; k = 4, 8, 12, \ldots \quad . \tag{3.3}$$

3.2 4-ary PSK

QPSK waveforms consist of two aligned modulation signals in phase quadrature. As with SQPSK the absolute phase of the ω carrier waveform does not affect the crosstalk formulas. In SQPSK the quadrature modulation waveform was shifted by T, or half the 4-ary signaling interval 2T for QPSK, where $R = 1/T$ is the data rate in bits per sec. An optimal AWGN receiver for QPSK is identical to that of Fig. 2.2 except that both demodulation channels use the same integration interval $(2nT, 2(n + 1)T)$ and sample at the same time $2(n + 1)T$.

For the same orthogonal center frequency spacings of $k/4T$, $k = 4, 8, 12, \ldots$, QPSK and SQPSK yield identical worst-case degradations. Orthogonal spacings of $k/4T$, $k = 2, 4, 6, \ldots$ are also possible for QPSK but the same degradation formula applies. That is, for the four possible cases for changes of sign in the interfering signal

Case 0: no change in a_n and no change in b_n at τ

Case 1: no change in a_n and change in b_n at τ

Case 2: change in a_n and no change in b_n at τ

Case 3: change in a_n and change in b_n at τ

the center frequency constraint, cf. Eq. (2.3)

$$\Delta T = \pi k', \quad k' = 1, 2, 3,... \tag{3.4}$$

guarantees no SNR degradation for $\tau = 0$. The QPSK crosstalk is

$$S_k(A,\lambda) = \frac{4\sqrt{2}\, A\lambda}{\pi k}, \quad k = 2, 4, 6,... \quad . \tag{3.5}$$

3.3 Alternating QPSK (AQPSK)

AQPSK, sometimes called quadrature advance/retard keying [10], is like offset QPSK except that the modulation waveform on each of the quadrature channels are three-valued as follows (see Fig. 1.2):

1) $\cos \omega t$ is modulated by the rectangular waveform assuming the values $a_n = \pm 1$ in the intervals $[2nT, (2n + 1)T)$ with transitions at $2nT$, and by the zero waveform in the intervening intervals $[(2n + 1)T, 2(n + 1)T)$; and

2) $\sin \omega t$ is modulated by $b_n = \pm 1$ in $[(2n - 1)T, 2nT)$ with transitions at $(2n - 1)T$, and by zero in the intervals $[2nT, (2n + 1)T)$.

An optimal AWGN receiver for AQPSK is identical to that of Fig. 2.2 except that the $\cos \omega t$ channel is sampled at $(2n + 1)T$ and the $\sin \omega t$ channel is sampled at $2nT$. Bit error performance is the same as that for BPSK.

Without loss of generality, one need consider only the $\cos \omega t$ demodulation channel and $t, \tau \in [0,T)$. The phase of the received ω term does not affect the crosstalk formula since only differences in trigonometric arguments are involved. Applying Eqs. (2.2) and (2.3) one obtains the normalized crosstalk

$$\frac{AR}{\omega-\nu}\left(\pm(\cos(\omega\tau-\theta)-\cos(\nu\tau-\theta))\ \mp\ (\sin(\omega\tau-\theta)-\sin(\nu\tau-\theta))\right).$$

Noting that this is $C_1(\tau, \theta) - C_2(\tau, \theta)$, or nearly the same as Eq. (2.5d) for Case 3 of SQPSK, the same formula

$$S_k(A, \lambda) = \frac{4\sqrt{2}\ A\lambda}{\pi k}, \quad k = 4, 8, 12,...$$

as Eq. (2.16) holds. However, the probability $P(\lambda)$ with which $S_k(A, \lambda)$ is exceeded for AQPSK is precisely $4P_3(\lambda)$, where $P_3(\lambda)$ is the SQPSK Case 3 probability, or $2P_1(\lambda)$, where $P_1(\lambda)$ is the BPSK Case 1 probability. Hence, $E(\hat{\lambda}) = \hat{\lambda} = 1$ and $E(\bar{\lambda}) = \bar{\lambda}/2 \doteq 0.2025$, twice the values for BPSK.

3.4 Minimum Shift Keying

MSK is the same as SQPSK except that a half cycle sine wave rather than a rectangular pulse of duration 2T is used to shape each modulation waveform. An optimal MSK receiver is the same as that of Fig. 2.2 except that cos ωt is replaced by cos $\omega_1 t$ − cos $\omega_2 t$ and sin ωt is replaced by cos $\omega_1 t$ + cos $\omega_2 t$, say, where ω_1 and ω_2 are the two signaling frequencies as defined below. Performance of the two systems in AWGN is identical.

A peak switching MSK waveform can be expressed as $\pm$ cos $\omega_{1,2} t$ in a given chip interval $nT \leq t \leq (n + 1)T$, $n = 0, \pm 1, \pm 2,...$, where

$$\omega_{1,2} := \omega_o \mp \delta \tag{3.6a}$$

$$\omega_o := \delta k_\omega, \ k_\omega := 3, 5, 7,... \tag{3.6b}$$

$$\delta := \frac{\pi}{2T} \quad . \tag{3.6c}$$

A frequency change at nT is accompanied by a sign change if, and only if, n is odd since phase is continuous and because the frequency difference is a half cycle per chip.

The received waveform now has the form

$$r(t) = \pm \cos \omega_{1,2} t \pm A \cos \left(\nu_{1,2} (t - \tau) + \theta\right) \tag{3.7}$$

where

$$\nu_{1,2} := \nu_o \mp \delta \tag{3.8a}$$

$$\nu_o := \delta k_\nu, \; k_\nu := 7, 9, 11, \ldots \tag{3.8b}$$

$$k := k_\nu - k_\omega, \; k = 4, 6, 8, \ldots \quad . \tag{3.8c}$$

The center frequency constraint

$$(\nu_o - \omega_o)T = \frac{\pi k}{2}, \quad k = 4, 6, 8, \ldots \tag{3.9}$$

reflects the minimal frequency spacing possible while maintaining mutual chip orthogonality for $\tau = 0$ at the four distinct signaling frequencies $\omega_1 < \omega_2 < \nu_1 < \nu_2$. This minimal spacing is depicted in Fig. 3.1.

Performing the multiplication for the upper demodulation channel

$$\begin{aligned} r(t) \; (\cos \omega_1 t - \cos \omega_2 t) = \pm 1/2 \; & (\cos(\omega_\ell - \omega_1) \; t - \cos(\omega_\ell - \omega_2)t) \\ & \pm \frac{A}{2} \left(\cos((\nu_m - \omega_1)t - \nu_m \tau + \theta) - \cos((\nu_m - \omega_2)t - \nu_m \tau + \theta)\right) \\ & \ell, \, m \varepsilon \{1,2\} \end{aligned} \tag{3.10}$$

where the choices of sign and frequency are independent. As with the previous modulation schemes, it does not matter what the absolute phase of the MSK ω

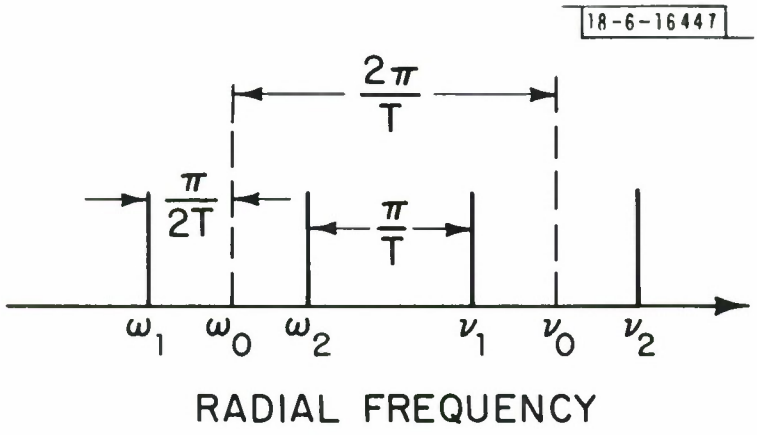

Fig. 3.1. Minimal orthogonal frequency spacing for MSK.

waveform is at t = 0 because the crossterms depend only on the cosine of the difference of the arguments in a cosine product. In particular, this means that peak switching MSK waveforms have the same crosstalk performance as zero crossing switching MSK waveforms. The ω_ℓ terms of Eq. (3.10) integrate to $\mp (-1)^\ell T$, $\ell = 1, 2$. There are four possible cases to consider with respect to the frequency changes in the interfering waveform at $t = \tau$ and $t = T + \tau$:

Case 0: no change at τ and no change at $T + \tau$

Case 1: no change at τ and change at $T + \tau$

Case 2: change at τ and no change at $T + \tau$

Case 3: change at τ and change at $T + \tau$.

The normalized MSK crosstalk formulas are

$$C_0(\tau, \theta) = 0 \tag{3.11a}$$

$$C_1(\tau, \theta) = \mp \frac{8A}{\pi k(k^2-4)} \left[\frac{k}{2} \sin (\nu_o\tau - \theta) \cos \delta\tau - \cos (\nu_o\tau - \theta) \sin \delta\tau \right.$$

$$\left. + (-1)^{k/2} \left[\frac{k}{2} \sin (\omega_o\tau - \theta) \cos \delta\tau + \cos (\omega_o\tau - \theta) \sin \delta\tau\right]\right] \tag{3.11b}$$

$$C_2(\tau, \theta) = \mp \frac{(-1)^m 8A}{\pi k(k^2-4)} \left[\left(\sin (\omega_o\tau - \theta) - \sin (\nu_o\tau - \theta)\right) \cos \delta\tau \right.$$

$$\left. + \frac{k}{2} \left(\cos (\omega_o\tau - \theta) + \cos (\nu_o\tau - \theta)\right) \sin \delta\tau\right] \tag{3.11c}$$

$$C_3(\tau, \theta) = C_1(\tau, \theta) + C_2(\tau, \theta) \quad . \tag{3.11d}$$

It is not difficult to show that $P_1(\lambda) = P_2(\lambda)$ with the maximal magnitude of the trigonometric factor of $C_1(\tau, \theta)$ and $C_2(\tau, \theta)$ equal to k for k/2 even

and approximately $k - 1$ for $k/2$ odd. Similarly, $P_3(\lambda)$ is the same for $k/2$ even and $m = 1$ or $m = 2$ in $C_3(\tau, \theta)$ with the maximal magnitude of the trigonometric factor equal to k. However, for $k/2$ odd the P_3 curve for $m = 2$ appears to be the same as that for $m = 1$ except that λ is replaced by $(k - 1)\lambda/(k + 1)$. In this instance the maximal magnitude of the trigonometric factor is approximately $k + 1$ for $m = 1$ and $k - 1$ for $m = 2$. Some experimental curves for $P_i(\lambda)$ are shown in Fig. 3.2.

For MSK, $p_i = 1/4$, $i = 0, 1, 2, 3$, as with SQPSK, but C_{max} depends on k, the parity of $k/2$ and m, the frequency index of the interfering waveform, while for SQPSK C_{max} just depended on k. For MSK, $\hat{\lambda}_0 = 0$ and for $k = 4, 6, 8, \ldots$

$$\hat{\lambda}_1 = \hat{\lambda}_2 = \begin{cases} 1, & k/2 \text{ even} \\ \approx \dfrac{k-1}{k+1}, & k/2 \text{ odd} \end{cases} \tag{3.12a}$$

$$\hat{\lambda}_3 = \begin{cases} 1, & k/2 \text{ even} \\ \left.\begin{array}{ll} 1, & m = 1 \\ \dfrac{k-2}{k+2}, & m = 2 \end{array}\right\}, & k/2 \text{ odd} \end{cases} \tag{3.12b}$$

$$E(\hat{\lambda}_i) = \begin{cases} \dfrac{3}{4}, & k/2 \text{ even} \\ \left.\begin{array}{ll} \approx \dfrac{3k-1}{4(k+1)}, & m = 1 \text{ in Case 3} \\ \approx \dfrac{3k^2+k-6}{4(k+1)(k+2)}, & m = 2 \text{ in Case 3} \end{array}\right\}, & k/2 \text{ odd} \end{cases} \tag{3.12c}$$

The mean values of λ and $E(\overline{\lambda}_i)$ are shown in Table 3.1 for $k = 4$, 6, 8 and 10.

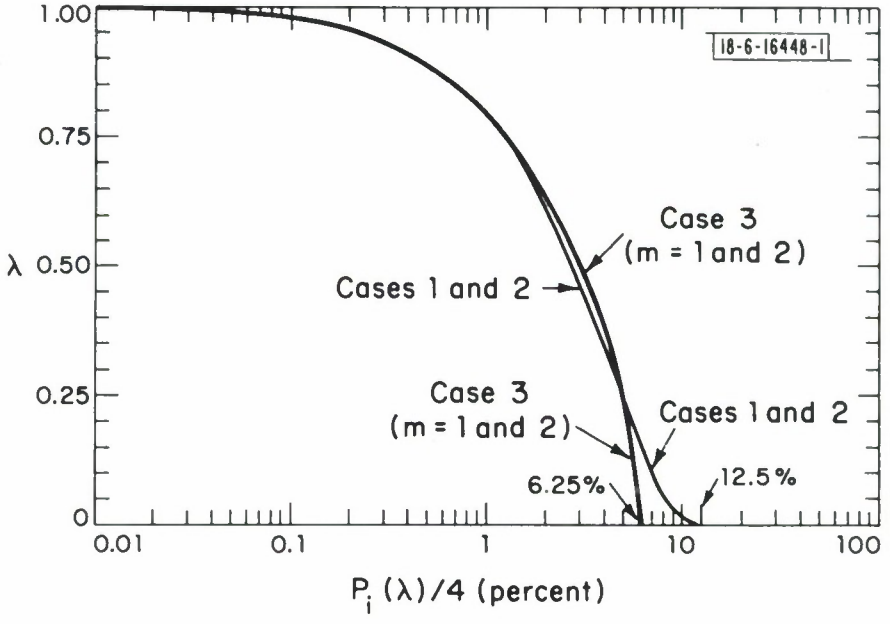

(a) k = 4.

Fig. 3.2. MSK crosstalk probabilities, Cases i = 1, 2, 3.

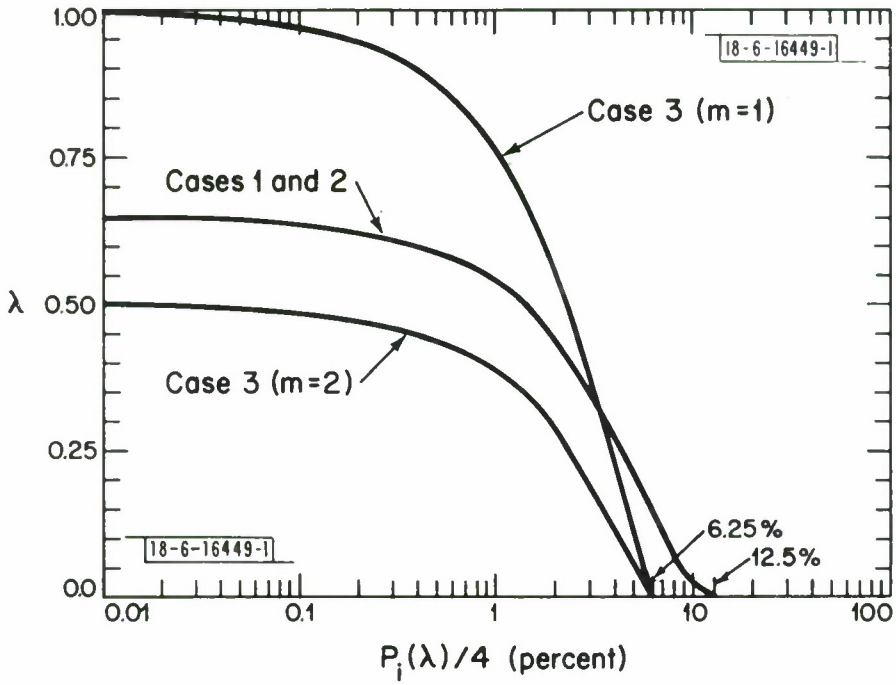

(b) k = 6.

Fig. 3.2. Continued.

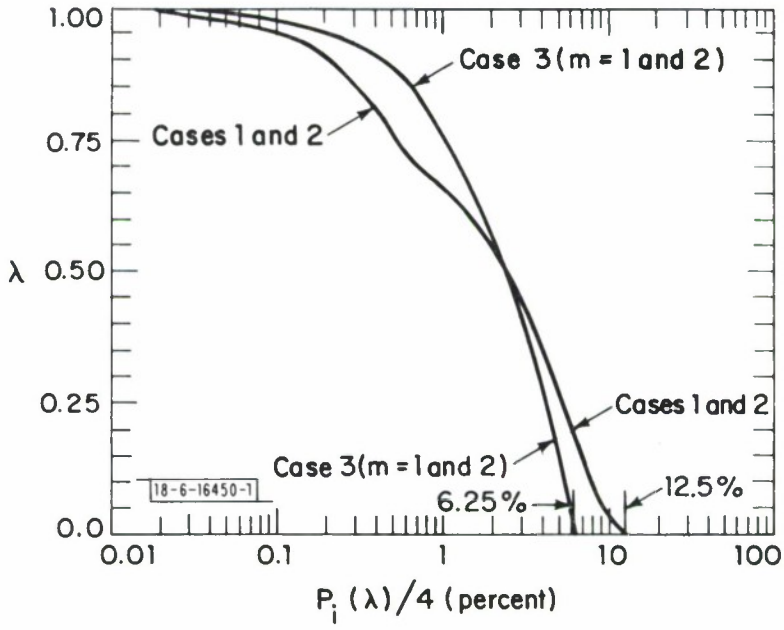

(c) k = 8.

Fig. 3.2. Continued.

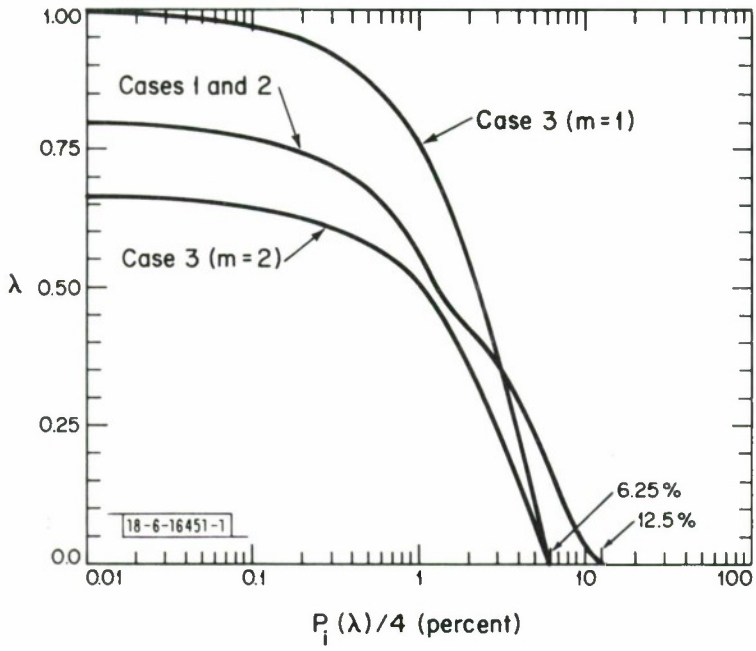

(d) k = 10.

Fig. 3.2. Continued.

TABLE 3.1

MEAN VALUES OF λ FOR MSK

k =	4	6	8	10
$\bar{\lambda}_1 = \bar{\lambda}_2 \doteq$	0.272	0.203	0.268	0.221
$\bar{\lambda}_3$ (m = 1) $\doteq$	0.487	0.407	0.432	0.404
$\bar{\lambda}_3$ (m = 2) $\doteq$		0.202		0.267
$E(\bar{\lambda}_i)$ (m = 1 in Case 3) $\doteq$	0.129	0.102	0.121	0.106
$E(\bar{\lambda}_i)$ (m = 2 in Case 3) $\doteq$		0.076		0.089

The MSK crosstalk formula, which is exceeded with probability $P(\lambda)$, is given by

$$S_k(A, \lambda) = \begin{cases} \dfrac{8(k+1)\,A\lambda}{\pi k(k^2-4)}, & k = 6, 10, 14, \ldots \\ \dfrac{8A\lambda}{\pi(k^2-4)}, & k = 4, 8, 12, \ldots \end{cases} \quad . \tag{3.13}$$

The formula holds only approximately for k/2 odd.

IV. CONTINUOUS-PHASE QUADRIFREQUENCY SHIFT KEYING (CPQFSK)

Thus far, the modulation schemes considered include both binary and 4-ary PSK and binary continuous-phase FSK. In this section the crosstalk formulas for 4-ary continuous-phase FSK are computed. But first an optimal coherent receiver for CPQFSK in the presence of AWGN is established.

4.1 Optimal Coherent CPQFSK Receiver

An optimal CPQFSK receiver in the presence of AWGN is shown in Fig. 4.1. Except for the two functions used for crosscorrelation, CPQFSK processing is identical to that of a QPSK receiver.

The upper demodulation channel of Fig. 4.1 is the same as that for the MSK receiver of Section 3.3 except that there the MSK crosscorrelating function was

$$\cos \omega_1 t - \cos \omega_2 t = 2 \sin \frac{\pi t}{2T} \sin \omega_o t \quad . \tag{4.1}$$

Since the peak switching CPQFSK waveform can be expressed as $\pm \cos \omega_i t$ in a given chip interval $2nT \leq t \leq 2(n + 1)T$, where

$$\omega_i := \omega_o + k(i)\delta \tag{4.2a}$$

$$\omega_o := \delta k_\omega, \quad k_\omega := 5, 7, 9, \ldots \tag{4.2b}$$

$$k(i) := 2i - 5, \quad i \in \{1, 2, 3, 4\} =: J \tag{4.2c}$$

$$\delta := \frac{\pi}{4T} \tag{4.2d}$$

$$(\omega_r - \omega_i)2T = (r - i)\pi, \quad r, i \in J \tag{4.2e}$$

the corresponding CPQFSK crosscorrelating function is

$$+ \cos \omega_1 t + \cos \omega_2 t - \cos \omega_3 t - \cos \omega_4 t$$

$$= 2 \left(\sin \frac{\pi t}{4T} + \sin \frac{3\pi t}{4T} \right) \sin \omega_o t \quad . \tag{4.3}$$

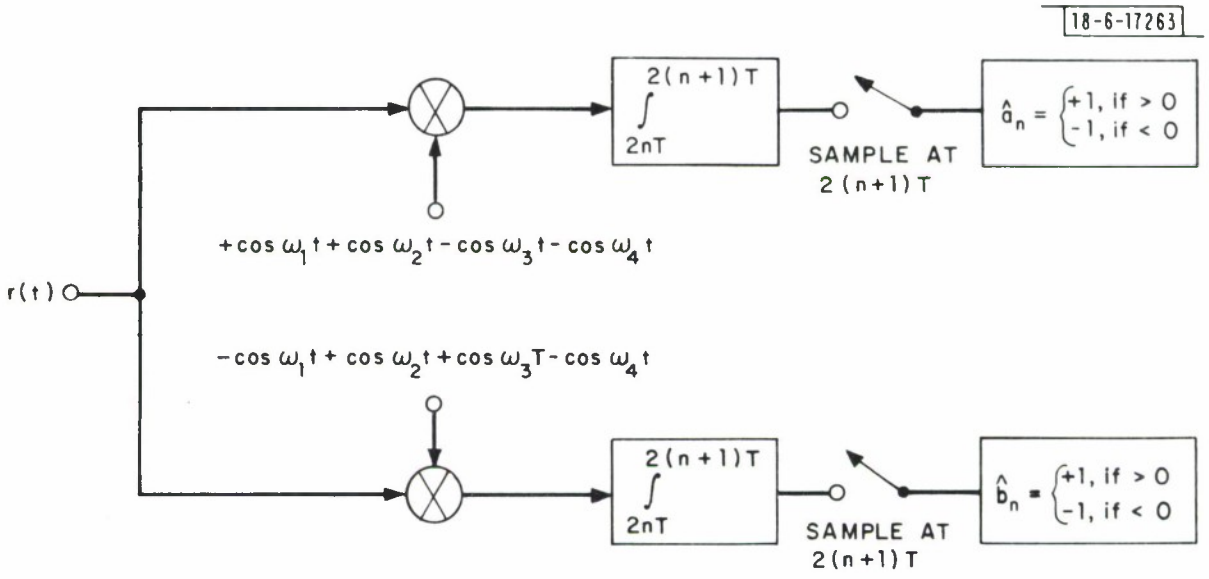

Fig. 4.1. Continuous-phase QFSK receiver.

Similarily, in the quadrature channel the crosscorrelating functions are

$$\cos \omega_1 t + \cos \omega_2 t = 2 \cos \frac{\pi t}{2T} \cos \omega_o t \tag{4.4}$$

for MSK and

$$-\cos \omega_1 t + \cos \omega_2 t + \cos \omega_3 t - \cos \omega_4 t$$

$$= 2 \left(\cos \frac{\pi t}{4T} - \cos \frac{3\pi t}{4T} \right) \cos \omega_o t \tag{4.5}$$

for CPQFSK.

Since by Eq. (4.2) the transmitted CPQFSK signal has the form

$$\pm \cos \omega_i t = \pm \cos \delta t \cos \omega_o t \pm \sin \delta t \sin \omega_o t$$

or $\pm \cos 3\delta t \cos \omega_o t \pm \sin 3\delta t \sin \omega_o t$

by Eq. (4.3) the upper channel effectively demodulates either

$$\pm \sin \delta t \text{ or } \pm \sin 3\delta t$$

while by Eq. (4.5) the quadrature channel effectively demodulates

$$\pm \cos \delta t \text{ or } \mp \cos 3\delta t \quad .$$

Thus, in the absence of noise and ignoring the double frequency terms, the output of each channel is $\pm$ T, and the performance of antipodal signals in AWGN is achieved, as with MSK, QPSK, BPSK and offset QPSK.

A state diagram for CPQFSK is shown in Fig. 4.2. If $k_\omega \equiv 3 \pmod 4$, the ω_1's and ω_3's of the transitions would be interchanged with the ω_2's and ω_4's. From each state there are 4 possible frequencies that can be transmitted in the next 2T sec, i.e., 2 bits of information a_n and b_n are sent at epoch n. Referring to Figs. 4.1 and 4.2, suppose that $a_n = +1$ and $b_n = -1$. This means that either $+\cos \omega_1 t$ or $-\cos \omega_3 t$ is transmitted.

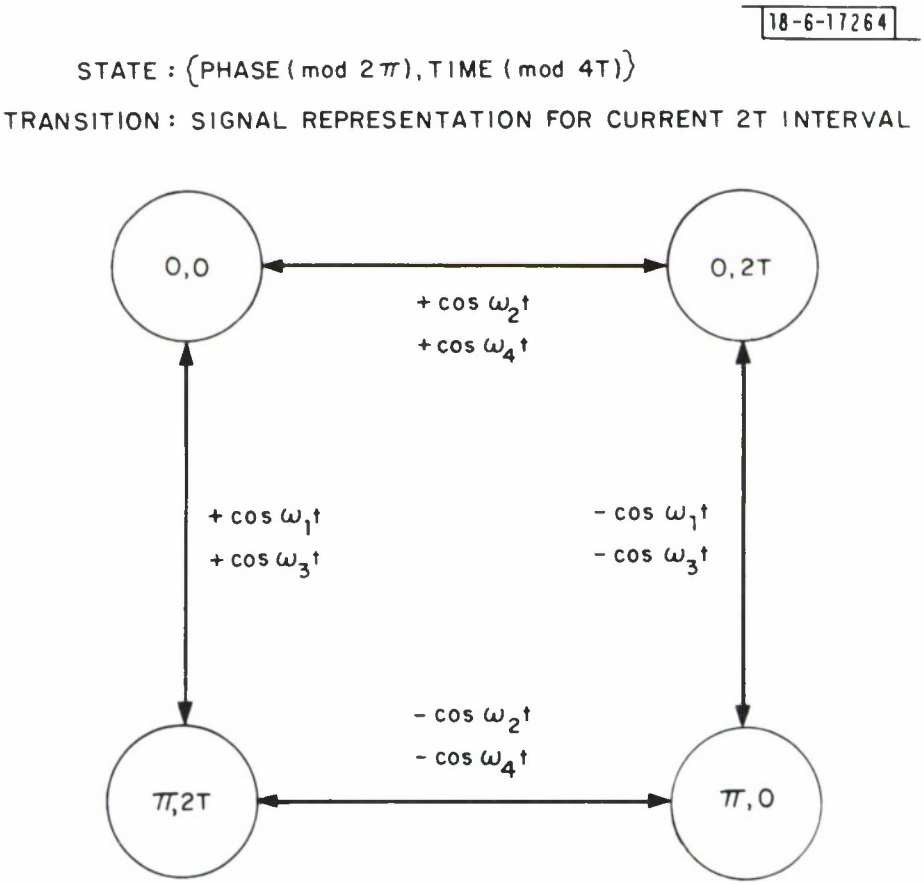

Fig. 4.2. State diagram for peak switching CPQFSK and $k_\omega \equiv 1 \pmod 4$.

The cosine transmitted is determined by the current state. For example, from state (0, 0), + cos $\omega_1 t$ must be sent while from state (π, 0), -cos $\omega_3 t$ must be sent. It can be verified that this works for any of the 4 possible values for $\{a_n, b_n\} = \{\pm 1, \pm 1\}$ and any of the 4 possible states, i.e., the binary-valued $\{a_n\}$ and $\{b_n\}$ data streams can be selected independently while maintaining phase continuity and transmitting one of 4 possible frequencies from each state.

4.2 Crosstalk Formulas

In the absence of noise the received waveform from two CPQFSK users has the form

$$r(t) = \pm \cos \omega_r t \pm A \cos \left(\nu_s (t - \tau) + \theta\right), \quad r, s \in J \tag{4.6}$$

where

$$\nu_j := \nu_o + k(j)\delta \tag{4.7a}$$

$$\nu_o := \delta k_\nu, \qquad k_\nu := 13, 15, 17, \ldots \tag{4.7b}$$

$$k(j) := 2j - 5, \qquad j \in J \tag{4.7c}$$

$$(\nu_s - \nu_j)2T = (s - j)\pi, \quad s, j \in J \tag{4.7d}$$

$$2k := k_\nu - k_\omega, \qquad k = 4, 5, 6, \ldots \quad . \tag{4.7e}$$

The center frequency constraint

$$(\nu_o - \omega_o)2T = \pi k, \quad k = 4, 5, 6, \ldots \tag{4.8}$$

reflects the minimal frequency spacing possible while maintaining mutual chip orthogonality for $\tau = 0$ at the eight distinct signal frequencies. This minimal spacing is depicted in Fig. 4.3. Note that the minimal center frequency spacing is identical to that of Fig. 3.1 for MSK and that the bandwidths occupied by the signaling frequencies are roughly the same.

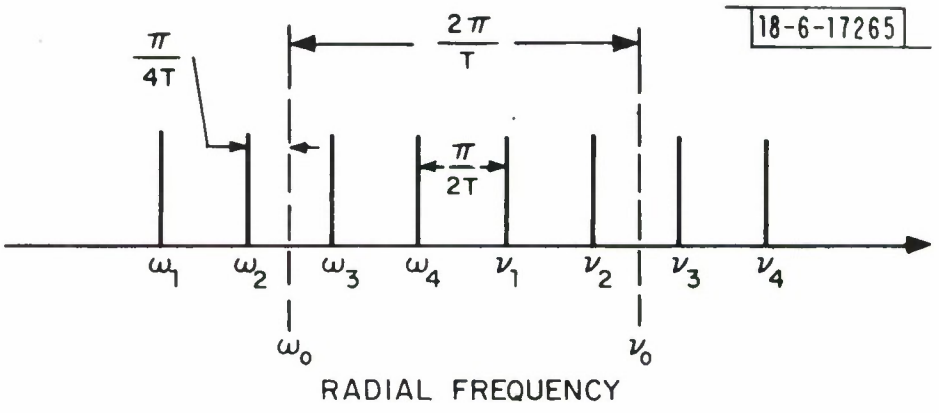

Fig. 4.3. Minimal orthogonal frequency spacing for CPQFSK.

Performing the multiplication for the upper demodulation channel

$$r(t)\left(\cos \omega_1 t + \cos \omega_2 t - \cos \omega_3 t - \cos \omega_4 t\right)$$

$$= \frac{1}{2} \sum_{j \in J} (-1)^{\left\lfloor \frac{j-1}{2} \right\rfloor} \left(\pm \cos(\omega_r - \omega_j)t \pm A \cos\left((\nu_s - \omega_j)t - \nu_s \tau + \theta\right)\right)$$

$$r, s \in J \qquad (4.9)$$

where the choices of sign and frequency are independent. Again, the absolute phase of the CPQFSK ω_r waveform is irrelevant from a crosstalk point of view. Hence, although continuous-phase switching is required, peak or zero crossing switching, for example, is unnecessary. The ω_r terms of Eq. (4.9) integrate to $\pm$ T, since by Eq. (4.2e)

$$\int_0^{2T} \cos\,(\omega_r - \omega_j)t\, dt = 2T\delta_{rj} \quad . \qquad (4.10)$$

For convenience in evaluating the contributions of the ν_s terms of the interfering user, the frequency indices $J = \{s, \bar{s}, s', \underline{s}\}$ are defined in Table 4.1. The crosstalk cases considered over the integration interval $[0,2T)$ are listed in Table 4.2, while the integrals over the appropriate subintervals are given in Table 4.3. Using the variables defined in Table 4.4 and the state diagram of Fig. 4.2, the results of the crosstalk calculations are listed in Table 4.5 as coefficients of the involved trigonometric products.

As one can see from Tables 4.4 and 4.5, worst-case CPQFSK crosstalk formulas are much more difficult to obtain than with MSK. However, some insight can be gained by considering each case individually and at least bounding the magnitude of the crosstalk function

TABLE 4.1

CYCLIC PERMUTATION GROUP OVER FREQUENCY INDICES J

·	e	—	′	—
e	e	—	′	—
—	—	e	—	′
′	′	—	e	—
—	—	′	—	e

Multiplication Table

s	$\bar{s}$	s′	$\underline{s}$
1	4	2	3
2	3	1	4
3	2	4	1
4	1	3	2

Mappings

TABLE 4.2

FREQUENCY INDICES OF INTERFERING SIGNAL FOR $[0, 2T)$

Case	$[0,\tau)$	$[\tau,2T)$
0	s	s
1	s	$\bar{s}$
2	s	s′
3	s	$\underline{s}$

TABLE 4.3

INTERFERENCE INTEGRALS OVER SUBINTERVALS

I Subinterval	$\frac{\pi}{2T}\int_I \cos((\nu_s - \omega_j)\ t - \nu_s\tau + \theta)\ dt$
$[0,\tau)$	$G_1(s,j) := \dfrac{\sin(\nu_s\tau - \theta) - \sin(\omega_j\tau - \theta)}{k+s-j}$
$[\tau,2T)$	$G_2(s,j) := \dfrac{\sin(\omega_j\tau - \theta) - (-1)^{k+s-j}\sin(\nu_s\tau - \theta)}{k+s-j}$

$$G(s,j) := G_1(s,j) + G_2(s,j) = \frac{(1 - (-1)^{k+s-j})\ \sin(\nu_s\tau - \theta)}{k+s-j}$$

TABLE 4.4

DEFINITION OF VARIABLES*

$$Z_j(\alpha) := \frac{1}{k+\alpha-j},\quad \alpha,\ j \in J$$

$$X_{ij}(\alpha,\beta) := Z_i(\alpha) + Z_j(\alpha) - (Z_i(\beta) + Z_j(\beta))$$

$$Y_{ij}(\alpha,\beta) := Z_i(\alpha) - Z_j(\alpha) - (Z_i(\beta) - Z_j(\beta))$$

$$(i,j) = (1,\ 4) \text{ or } (2,\ 3);\quad \alpha,\beta \in J,\ \alpha \neq \beta$$

$$U(\alpha) := Z_1(\alpha) - Z_2(\alpha) - (Z_3(\alpha) - Z_4(\alpha))$$

$$V(\alpha) := Z_1(\alpha) + Z_2(\alpha) - (Z_3(\alpha) + Z_4(\alpha))$$

, $\alpha \in J$

---

* For convenience the dependence of the constant k has been suppressed in the notation.

TABLE 4.5

COEFFICIENTS OF TRIGONOMETRIC PRODUCTS

Trigonometric Product Component of $\sum_{j\in J}(-1)^{\left\lfloor\frac{j-1}{2}\right\rfloor}{}_G$	Case 0 $G = G(s,j)$	Case 1 $G = G_1(s,j) + G_2(\bar{s},j)$	Case 2 $G = G_1(s,j) + G_2(s',j)$	Case 3 $G = G_1(s,j) + G_2(\underline{s},j)$
$\sin(\nu_o\tau-\theta)\cos\delta\tau$	$V(s)\underline{+}(-1)^k U(s)$, $s=2,3$	$V(s)\bar{+}(-1)^k U(\bar{s})$, $s=2,3$	$\left\{\begin{array}{l}\underline{+}(-1)^k U(s'),\ s=1,4\\ V(s),\ s=2,3\end{array}\right\}$	$\left\{\begin{array}{l}\bar{+}(-1)^k U(\underline{s}),\ s=1,4\\ V(s),\ s=2,3\end{array}\right\}$
$\sin(\nu_o\tau-\theta)\cos3\delta\tau$	$V(s)\bar{+}(-1)^k U(s)$, $s=1,4$	$V(s)\underline{+}(-1)^k U(\bar{s})$, $s=1,4$	$\left\{\begin{array}{l}V(s),\ s=1,4\\ \bar{+}(-1)^k U(s'),\ s=2,3\end{array}\right\}$	$\left\{\begin{array}{l}V(s),\ s=1,4\\ \underline{+}(-1)^k U(\underline{s}),\ s=2,3\end{array}\right\}$
$\cos(\nu_o\tau-\theta)\sin\delta\tau$	$\bar{+}V(s)-(-1)^k U(s)$, $s=2,3$	$\bar{+}V(s)-(-1)^k U(\bar{s})$, $s=2,3$	$\left\{\begin{array}{l}-(-1)^k U(s'),\ s=1,4\\ \bar{+}V(s),\ s=2,3\end{array}\right\}$	$\left\{\begin{array}{l}-(-1)^k U(\underline{s}),\ s=1,4\\ \bar{+}V(s),\ s=2,3\end{array}\right\}$
$\cos(\nu_o\tau-\theta)\sin3\delta\tau$	$\bar{+}V(s)+(-1)^k U(s)$, $s=1,4$	$\bar{+}V(s)+(-1)^k U(\bar{s})$, $s=1,4$	$\left\{\begin{array}{l}\bar{+}V(s),\ s=1,4\\ (-1)^k U(s'),\ s=2,3\end{array}\right\}$	$\left\{\begin{array}{l}\bar{+}V(s),\ s=1,4\\ (-1)^k U(\underline{s}),\ s=2,3\end{array}\right\}$
$\sin(\omega_o\tau-\theta)\cos\delta\tau$	0	$-Y_{23}(s,\bar{s})$	$-Y_{23}(s,s')$	$-Y_{23}(s,\underline{s})$
$\sin(\omega_o\tau-\theta)\cos3\delta\tau$	0	$-Y_{14}(s,\bar{s})$	$-Y_{14}(s,s')$	$-Y_{14}(s,\underline{s})$
$\cos(\omega_o\tau-\theta)\sin\delta\tau$	0	$X_{23}(s,\bar{s})$	$X_{23}(s,s')$	$X_{23}(s,\underline{s})$
$\cos(\omega_o\tau-\theta)\sin3\delta\tau$	0	$X_{14}(s,\bar{s})$	$X_{14}(s,s')$	$X_{14}(s,\underline{s})$

$$f(s,\tau,\theta) := \sum_{j\in J} (-1)^{\left\lfloor \frac{j-1}{2} \right\rfloor} G \quad . \tag{4.11}$$

Referring to Table 4.5, for Case 0, f can be expressed as

$$f_0(s,\tau,\theta) = \begin{cases} (V(s) \pm (-1)^k U(s)) \sin(v \mp t), & s = 2, 3 \\ (V(s) \mp (-1)^k U(s)) \sin(v \mp 3t), & s = 1, 4 \end{cases} \tag{4.12}$$

where the shorthand notation

$$t := \delta\tau \tag{4.13a}$$

$$v := \nu_o \tau - \theta \tag{4.13b}$$

has been used. It can be verified that

$$U(s) = \frac{2(2(k+s)-5)}{\prod_{j=1}^{4} (k+s-j)} = \begin{cases} \dfrac{2(2k-3)}{k(k-1)\ (k-2)\ (k-3)}, & s=1 \\ \dfrac{2(2k-1)}{k(k^2-1)\ (k-2)}, & s=2 \\ \dfrac{2(2k+1)}{k(k^2-1)\ (k+2)}, & s=3 \\ \dfrac{2(2k+3)}{k(k+1)\ (k+2)\ (k+3)}, & s=4 \end{cases} . \tag{4.14a}$$

where $U(s) > U(s+1) > 0$ for $k \geq 4$ and $s = 1, 2,$ and 3, and that

$$V(s)= \frac{-2(2(k+s)^2 - 10(k+s)+11)}{\prod_{j=1}^{4} (k+s-j)} = \begin{cases} \dfrac{-2(2k^2-6k+3)}{k(k-1)\ (k-2)\ (k-3)}, & s=1 \\ \dfrac{-2(2k^2-2k-1)}{k(k^2-1)\ (k-2)}, & s=2 \\ \dfrac{-2(2k^2+2k-1)}{k(k^2-1)\ (k+2)}, & s=3 \\ \dfrac{-2(2k^2+6k+3)}{k(k+1)\ (k+2)\ (k+3)}, & s=4 \end{cases} \tag{4.14b}$$

where $V(s) < V(s+1) < 0$ for $k \geq 4$ and $s = 1, 2,$ and 3. Note that $V(s) = O(k^{-2})$ while $U(s) = O(k^{-3})$. From Eq. (4.12) and these ordering properties of U and V, the Case 0 maximum is given by

$$\begin{aligned} |f_0(s,\tau,\theta)|_{\max} &= U(1) - V(1) \\ &= \frac{4}{(k-1)(k-3)} \sim \frac{4}{k^2} \end{aligned} \tag{4.15}$$

by Eq. (4.14). This maximum is achieved when $s = 1$, k is even, and $v - 3t \equiv \pi/2 \pmod{\pi}$. In other instances Eq. (4.15) serves as an upper bound to the magnitude of the Case 0 crosstalk function.

For Case 1, f can be expressed as

$$f_1(s,\tau,\theta) = f_{1v}(s,\tau,\theta) + f_{1\omega}(s,\tau,\theta) \tag{4.16a}$$

where

$$f_{1v}(s,\tau,\theta) := \begin{cases} V(s)\ \sin(v \mp t) \mp (-1)^k U(\bar{s})\ \sin(v \pm t) & , s = 2, 3 \\ V(s)\ \sin(v \mp 3t) \pm (-1)^k U(\bar{s})\ \sin(v \pm 3t), & s = 1, 4 \end{cases} \tag{4.16b}$$

and

$$f_{1\omega}(s,\tau,\theta) := (Z_3(s) - Z_3(\bar{s}))\ \sin(w + t) - (Z_2(s) - Z_2(\bar{s}))\ \sin(w - t) + (Z_4(s) - Z_4(\bar{s}))\ \sin(w + 3t) - (Z_1(s) - Z_1(\bar{s}))\ \sin(w - 3t) \tag{4.16c}$$

using the definitions of X_{ij} and Y_{ij} in Table 4.4 and the notation

$$w := \omega_o \tau - \theta \quad . \tag{4.17}$$

In this case an upper bound to $|f_1|$ is obtained by finding the extrema of $f_{1\nu}$ and $f_{1\omega}$ and adding their magnitudes.

It can be verified that U(4)-V(1) > U(3)-V(2) > U(2)-V(3) > U(1)-V(4) > 0 using Eq. (4.14). Thus, the maximum of the ν_o terms is given by

$$|f_{1\nu}(s,\tau,\theta)|_{\max} = U(4) - V(1) \ . \tag{4.18}$$

This maximum is achieved when s = 1, $v - 3t \equiv \pi/2 \pmod{\pi}$, and when τ = 2T/3 for k even, and when τ = 0 or 4T/3 for k odd, cf. Eqs. (4.2d) and (4.13a).

Now with regard to $f_{1\omega}$, from Table 4.4

$$Z_j(\alpha) - Z_j(\beta) = \frac{\beta - \alpha}{(k + \alpha - j)(k + \beta - j)} \ . \tag{4.19}$$

Observe that for every j, s = 1 or s = 4 achieves the maximum

$$\Delta\bar{Z}_j := \max_s |Z_j(s) - Z_j(\bar{s})| \tag{4.20}$$

using Table 4.1 and Eq. (4.19). Furthermore, $\Delta\bar{Z}_4 > \Delta\bar{Z}_3 > \bar{Z}_2 > \bar{Z}_1 > 0$. Thus, from Eq. (4.16c)

$$|f_{1\omega}(s,\tau,\theta)|_{\max} < \sum_{j\in J} \Delta\bar{Z}_j \tag{4.21}$$

and from Eqs. (4.16a), (4.18), (4.20) and (4.21) and Table 4.4

$$|f_1(s,\tau,\theta)|_{max} < 2(Z_3(1) + Z_4(1) - Z_2(4) - Z_3(4))$$

$$= \frac{8(2k^2 - 2k - 7)}{(k + 1)(k^2 - 4)(k - 3)} \sim \frac{16}{k^2} \quad . \tag{4.22}$$

Similarly, for Case 2 it can be shown that

$$|f_2(s,\tau,\theta)|_{max} < 2(Z_3(1) + Z_4(1) - Z_2(2) - Z_3(2))$$

$$= \frac{4(2k^2 - 6k + 3)}{k(k - 1)(k - 2)(k - 3)} \sim \frac{8}{k^2} \quad . \tag{4.23}$$

For Case 3 one can obtain the upper bound

$$|f_3(s,\tau,\theta)|_{max} < 2(Z_3(1) + Z_4(1) - Z_2(3) - Z_3(3))$$

$$= \frac{12(k^2 - 2k - 1)}{k(k + 1)(k - 2)(k - 3)} \sim \frac{12}{k^2} \quad . \tag{4.24}$$

On comparing Eqs. (4.15) and (4.22-24) for k = 4, 5, 6,... the upper bound to f becomes

$$|f(s,\tau,\theta)|_{max} < \frac{8(2k^2 - 2k - 7)}{(k + 1)(k^2 - 4)(k - 3)} \tag{4.25}$$

using the upper bound of Eq. (4.22) for Case 1. Hence, with the proper normalization of A/π from Eqs. (4.9) and (4.11) and Tables 4.3 and 4.5, the worst-case CPQFSK crosstalk is bounded by

$$C_{max} < \frac{8A(2k^2 - 2k - 7)}{\pi(k+1)(k^2-4)(k-3)}, \quad k = 4, 5, 6, \ldots \quad . \tag{4.26}$$

It can be shown that the bound of Eq. (4.15) for Case 0 is asymptotically (large k) tight for every s and k. For Cases 1, 2 and 3, one can also show that

$$|f_1(s,\tau,\theta)|_{max} \sim \frac{13+}{k^2}, \quad s = 1, 4 \tag{4.27a}$$

$$|f_2(s,\tau,\theta)|_{max} \sim \frac{7+}{k^2}, \quad s = 1, 2, 3, 4 \tag{4.27b}$$

$$|f_3(s,\tau,\theta)|_{max} \sim \frac{10+}{k^2}, \quad s = 1, 2, 3, 4 \tag{4.27c}$$

for some large k. Thus, the bounds obtained in Eq. (4.22)-(4.24) are reasonably tight. In particular, the Case 1 bound is about 1.2 times the worst-case crosstalk asymptotically. The ratio of the Case 1 bound to the actual worst-case crosstalk, cf. (4.26), calculated by a computer is plotted in Fig. 4.4 for k = 4 to 13. The ratio of this bound to its asymptote of $16A/\pi k^2$ is also shown.

Experimental curves of the actual CPQFSK crosstalks for a k = 4 threshold analysis are presented in Fig. 4.5. Although similar curves have been obtained for k = 5 to 8, they will not be shown. Instead, just the peak threshold for Cases 0 to 3 are depicted in Fig. 4.6. In all cases, s = 1 resulted in the largest crosstalk. This is to be expected since ν_1 is the interfering frequency closest to the ω frequencies, cf. Fig. 4.3 and Eq. (4.9). Furthermore, the worst-case crosstalk always resulted in Case 1 when the ν signaling frequency changed from ν_1 to ν_4, cf. Tables 4.1 and 4.2.

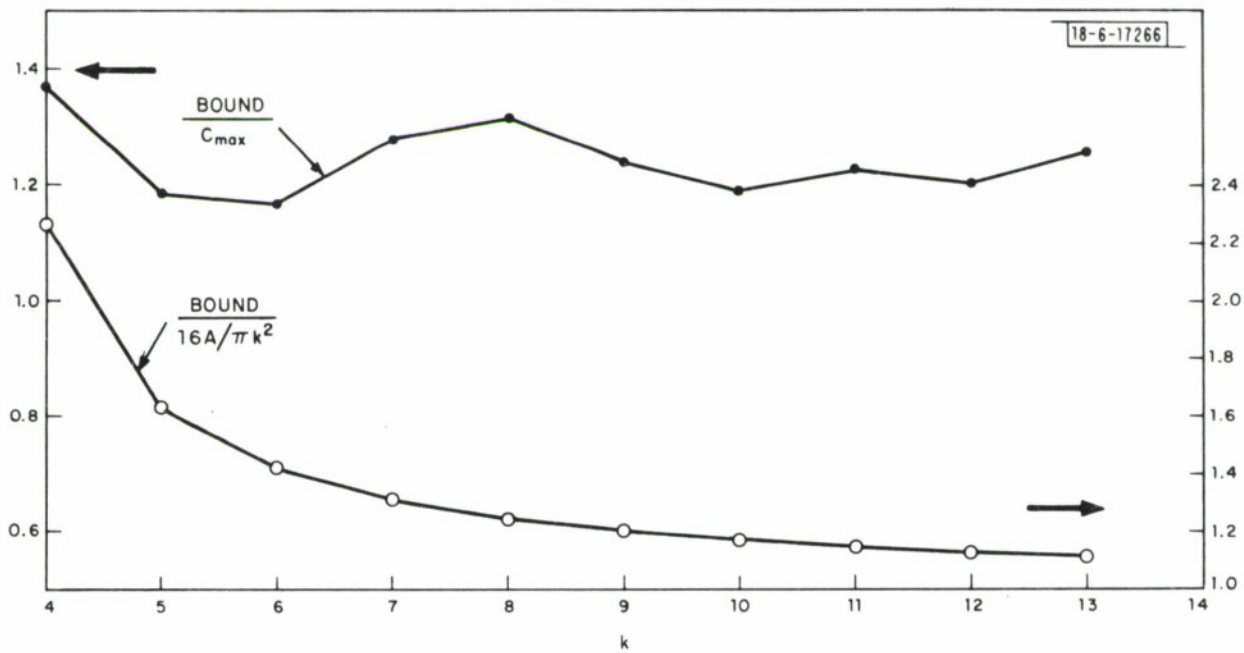

Fig. 4.4. Case 1 upper bound normalized by C_{max} and asymptote.

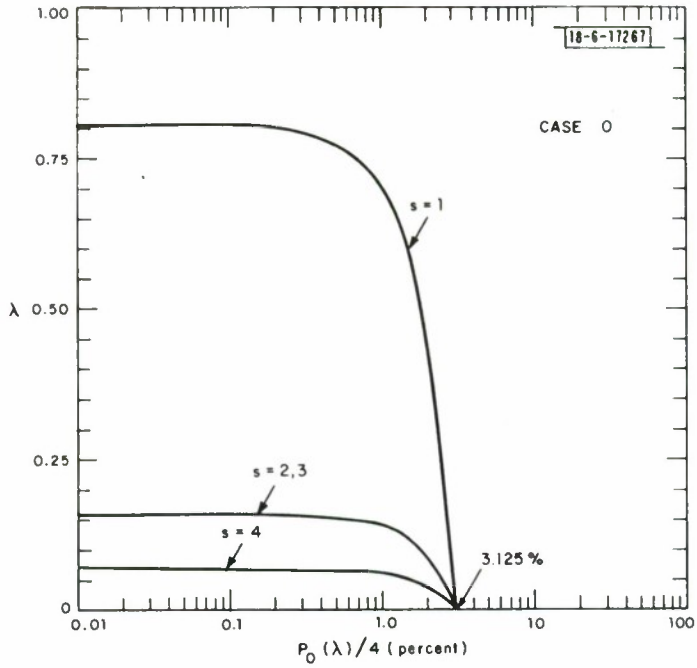

(a) Case 0.

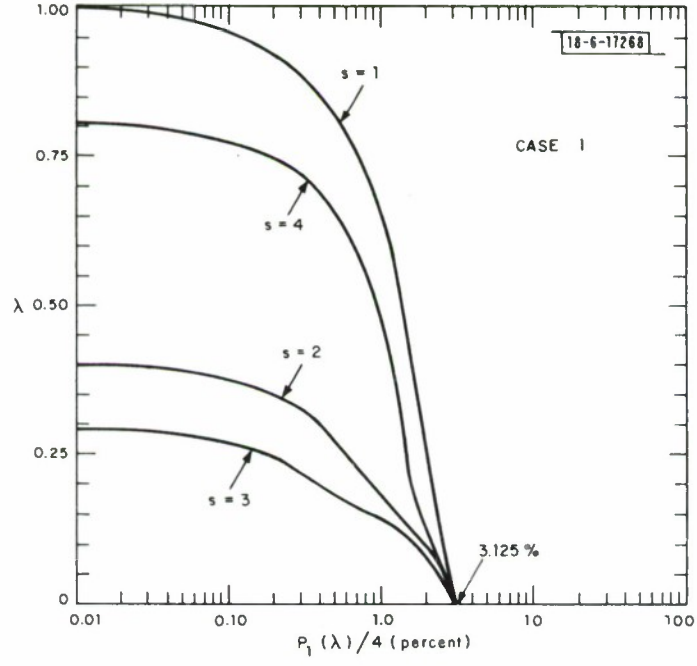

(b) Case 1.

Fig. 4.5. Crosstalk probabilities for CPQFSK, k = 4.

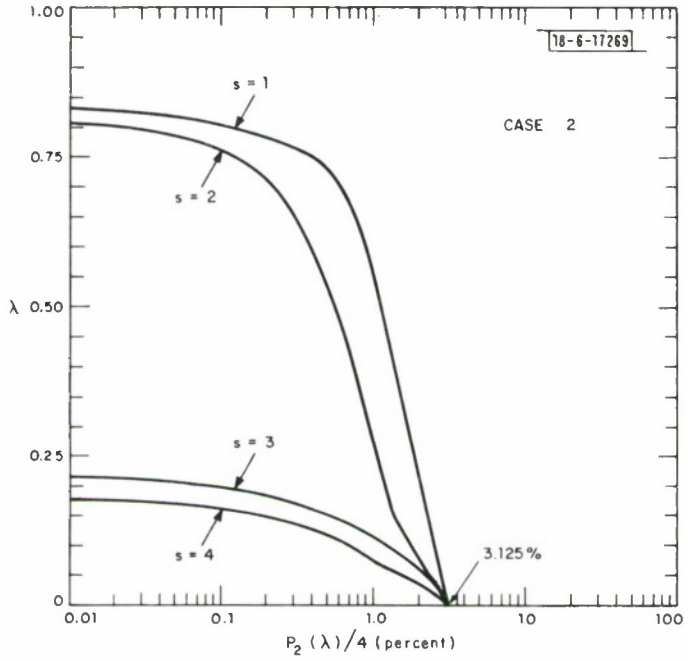

(c) Case 2.

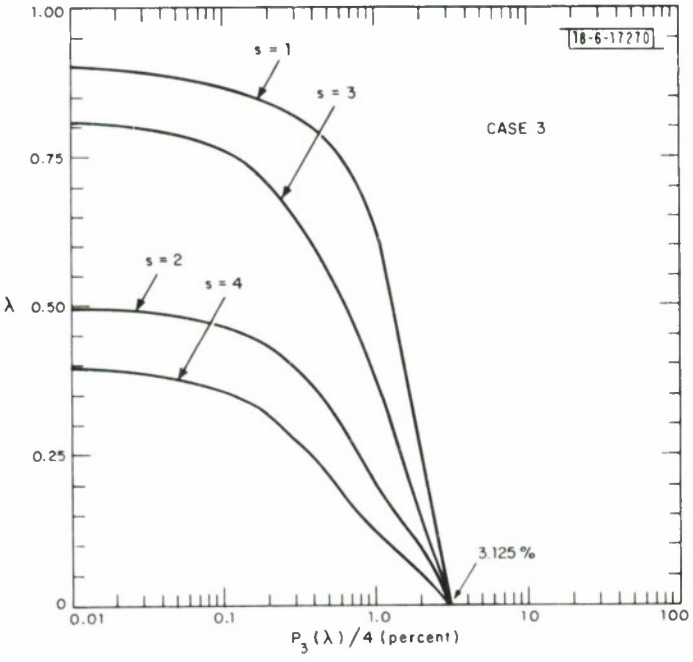

(d) Case 3.

Fig. 4.5. Continued.

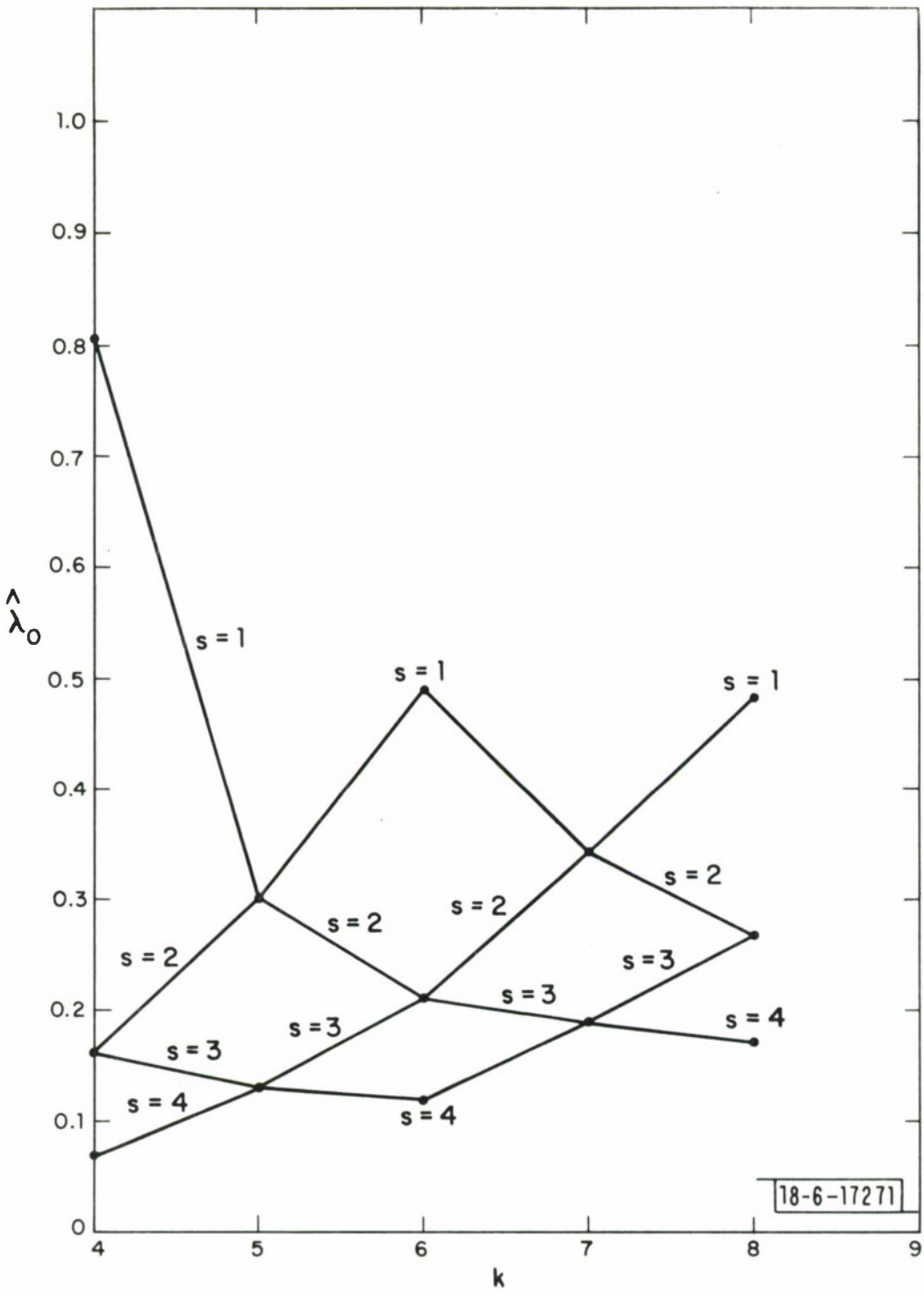

(a) Case 0.

Fig. 4.6. Peak CPQFSK thresholds for k = 4, 5, 6, 7, 8 and s = 1, 2, 3, 4.

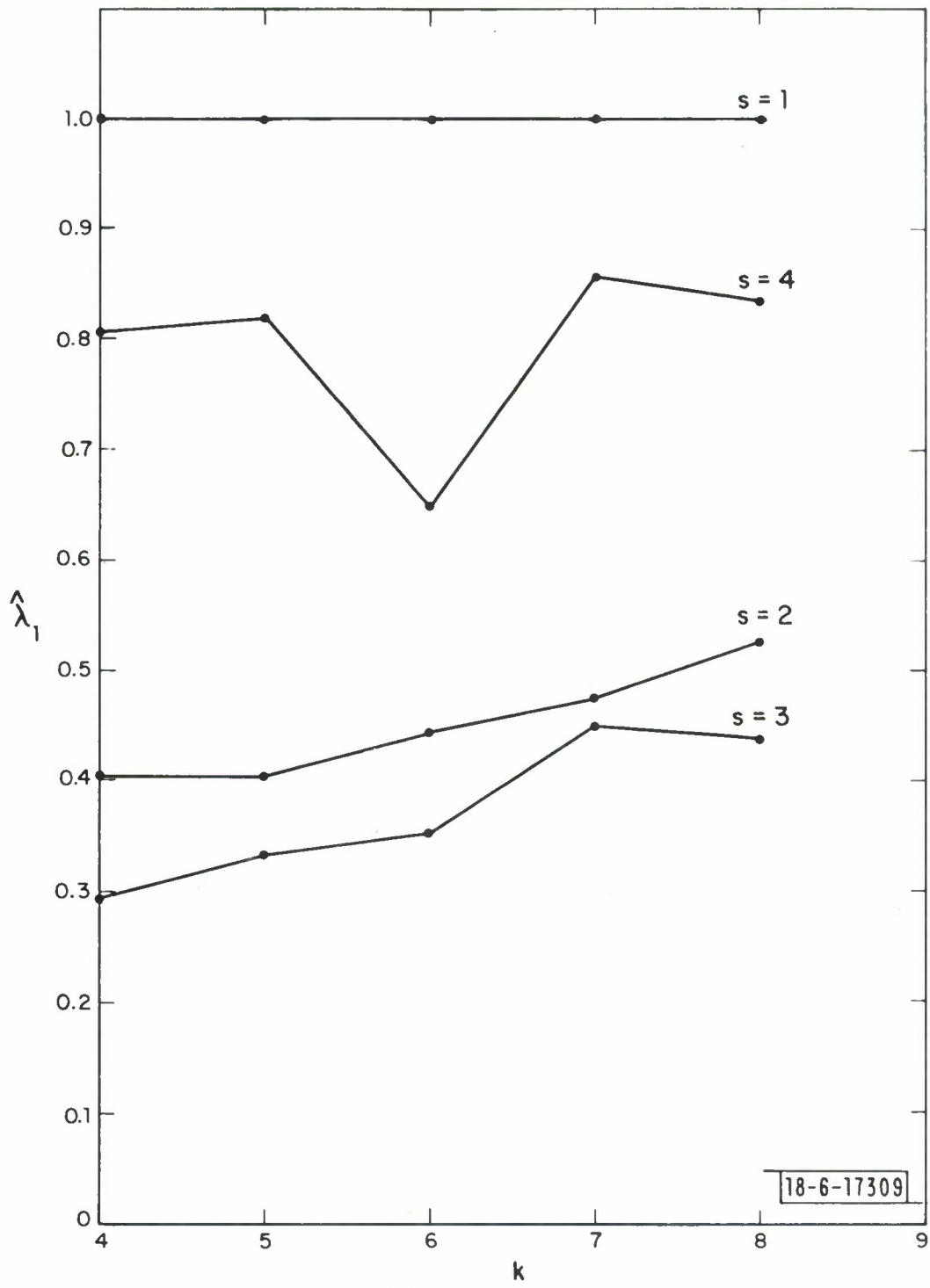

(b) Case 1.

Fig. 4.6. Continued.

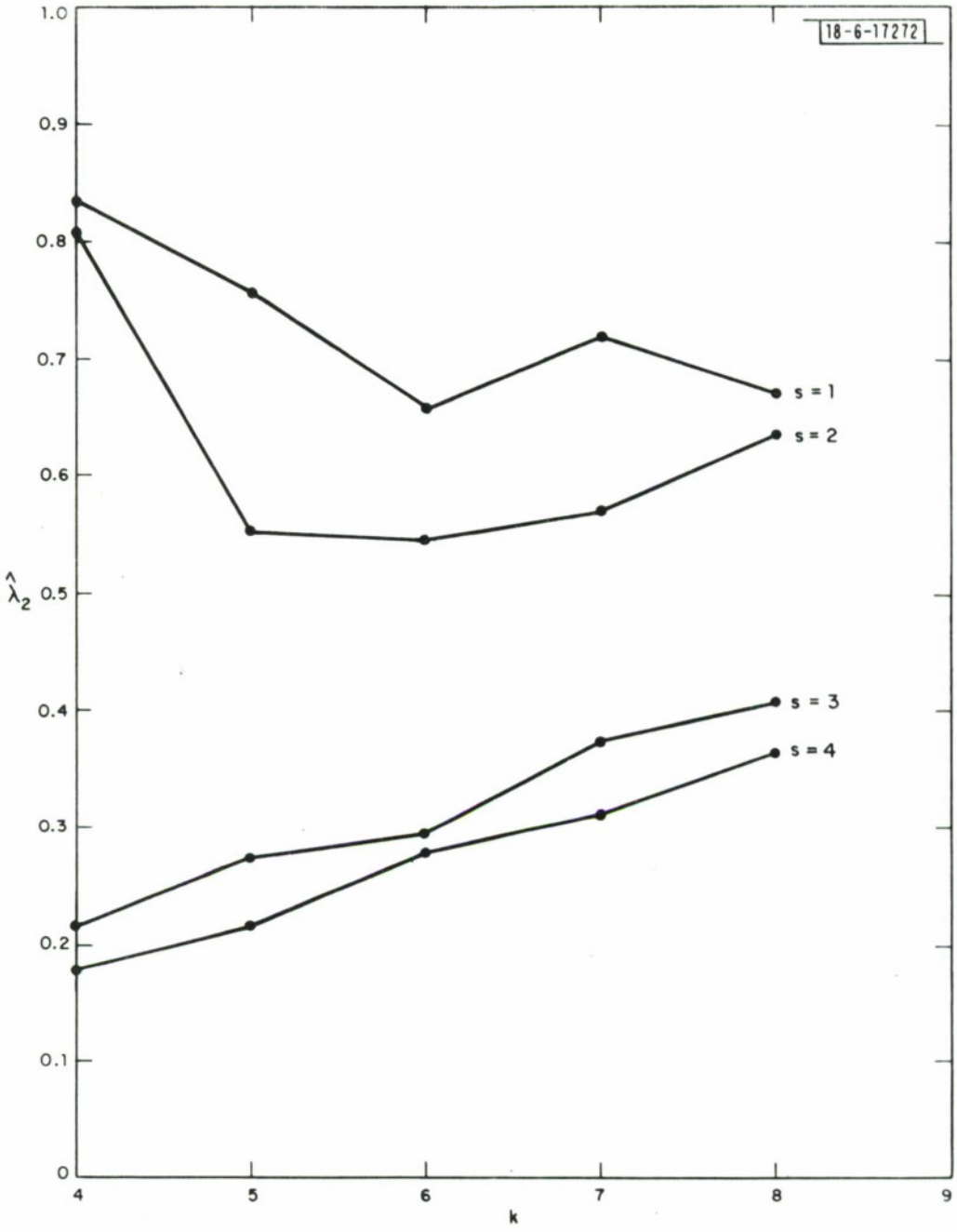

(c) Case 2.

Fig. 4.6. Continued.

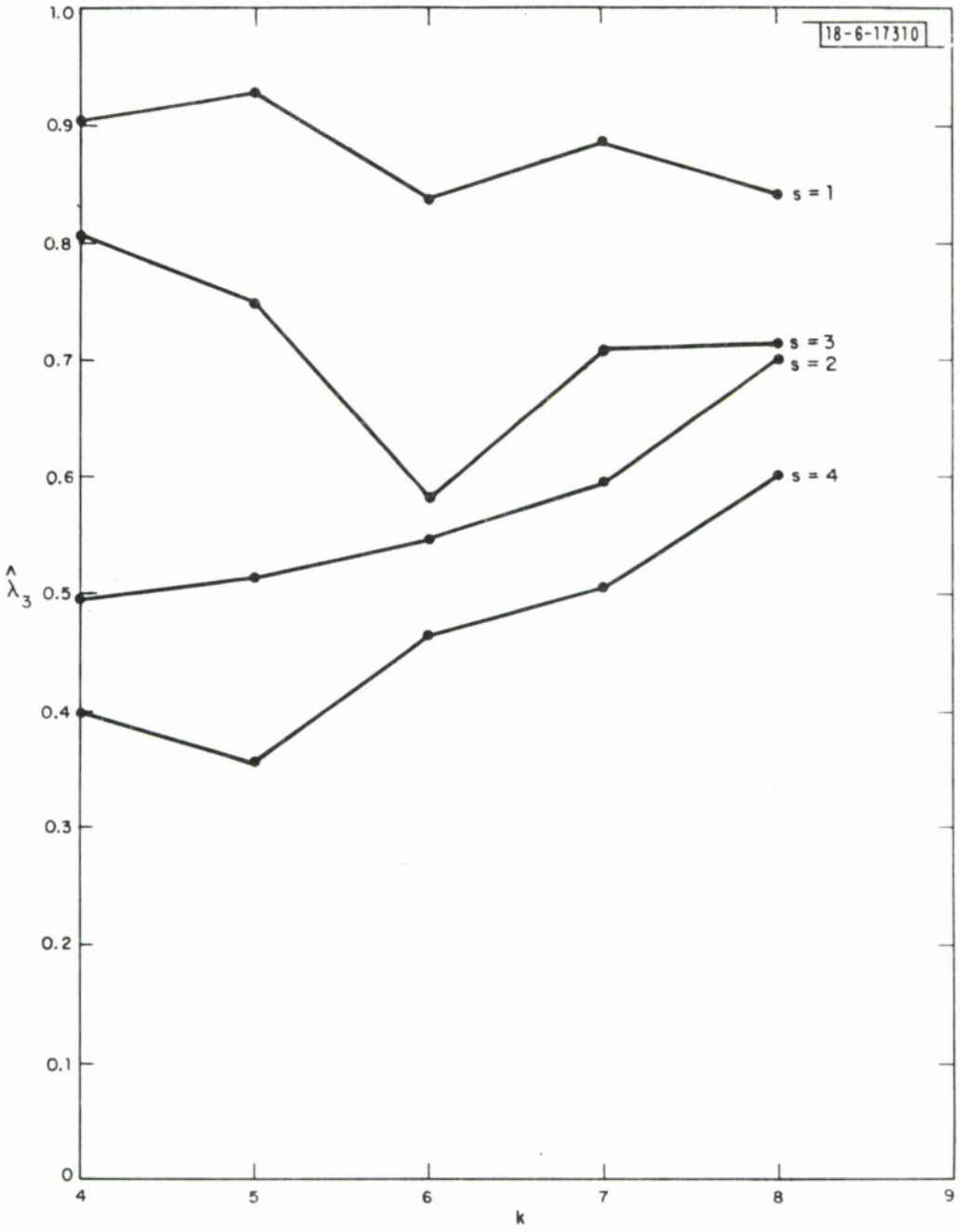

(d) Case 3.

Fig. 4.6. Continued.

V. CROSSTALK FOR 4-ARY BIORTHOGONAL FSK

The last modulation scheme treated in this report is 4-ary biorthogonal FSK. An optimal coherent receiver like that shown in Fig. 5.1 yields the same bit error probability in AWGN as all modems considered previously. Here the 4-ary biorthogonal signal set consists of non-continuous-phase peak-switching FSK chips with the data bits <——> chip correspondence

$$a_n b_n := \begin{cases} 00 \quad <\!\!\longrightarrow\!\!> \quad +\cos\omega_2 t \\ 11 \quad <\!\!\longrightarrow\!\!> \quad -\cos\omega_2 t \\ 01 \quad <\!\!\longrightarrow\!\!> \quad +\cos\omega_3 t \\ 10 \quad <\!\!\longrightarrow\!\!> \quad -\cos\omega_3 t \end{cases} .$$

This biorthogonal set requires just half the number of frequencies as CPQFSK, and thus, about half the bandwidth for minimally spaced frequencies. However, the spectrum of CPQFSK rolls off faster for larger deviations from the center frequency since phase is not continuous for these biorthogonal waveforms. With twice the minimum frequency spacing a biorthogonal set requires a bandwidth comparable to CPQFSK. However, this double spacing will probably be less competitive with respect to crosstalk performance than the original biorthogonal set. In any event, it will be interesting to compare the biorthogonal crosstalk formulas with those for CPQFSK.

In this section the analysis will be limited to finding worst-case crosstalk formulas, i.e., a threshold analysis like that of Section 2.2 will not be performed.

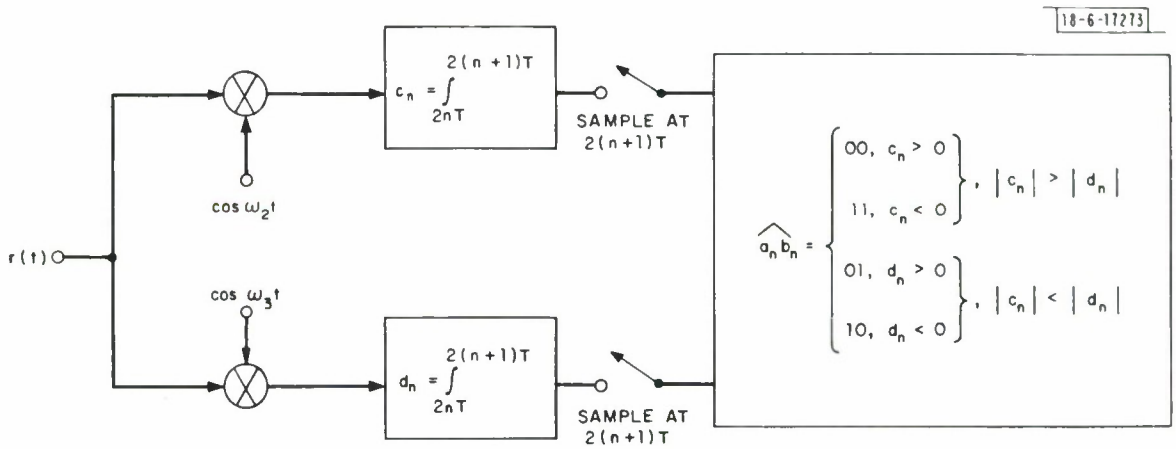

Fig. 5.1. 4-ary biorthogonal FSK receiver.

5.1 Minimal Orthogonal Spacing

The signaling frequencies for the minimal orthogonal spacing shown in Fig. 5.2 are defined by

$$\omega_{2,3} := \omega_o \mp \delta \tag{5.1a}$$

$$\omega_o := \delta k_\omega, \qquad k_\omega := 3, 5, 7, \ldots \tag{5.1b}$$

$$\delta := \frac{\pi}{4T} \tag{5.1c}$$

$$\nu_{2,3} := \nu_o \mp \delta \tag{5.1d}$$

$$\nu_o := \delta k_\nu, \qquad k_\nu := 7, 9, 11, \ldots \tag{5.1e}$$

$$2k := k_\nu - k_\omega, \qquad k = 2, 3, \ldots \quad . \tag{5.1f}$$

Referring to Figs. 5.1 and 5.2, it is evident that the worst-case crosstalk will occur in the ω_3 receiving channel since $\omega_o < \nu_o$. Therefore, the ω_2 receiving channel need not be considered.

The received waveform has the form

$$r(t) = \pm \cos\omega_{2,3}t \pm A \cos(\nu_{2,3}(t - \tau) + \theta), \quad 0 \leq \tau < 2T \quad . \tag{5.2}$$

For the lower demodulation channel of Fig. 5.1

$$r(t) \cos\omega_3 t = \frac{1}{2} \left(\pm \cos(\omega_r - \omega_3)t \pm A \cos((\nu_s - \omega_3)t - \nu_s\tau + \theta)\right) \tag{5.3}$$

where the signs and frequency indices r, s $\varepsilon\{2,3\}$ are independent. The contribution of the ω_r term is

$$\pm \frac{1}{2}\int_0^{2T} \cos(\omega_r - \omega_3)t \, dt = \pm T\delta_{r3} \quad . \tag{5.4}$$

The crosstalk calculations are summarized in Tables 5.1-5.3. By inspection

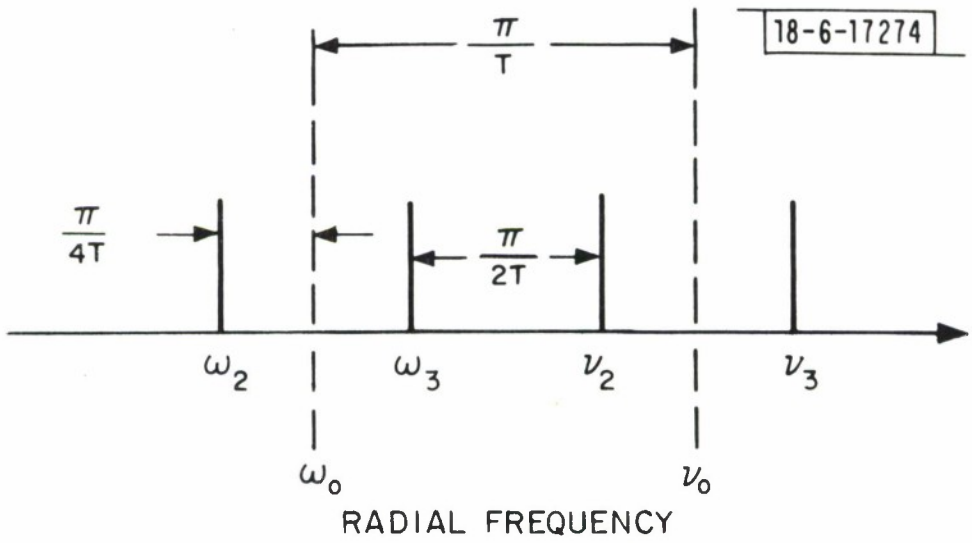

Fig. 5.2. Minimal orthogonal frequency spacing for biorthogonal FSK.

TABLE 5.1

CHARACTERIZATION OF INTERFERING WAVEFORM

Case	Change at $t = \tau$
0	none
1	sign but not frequency
2	frequency but not sign
3	both sign and frequency

$$\begin{matrix}(\nu_s - \omega_3)2T = (k + s - 3)\pi \\ (\nu_{\bar{s}} - \omega_3)2T = (k - s + 2)\pi\end{matrix}, \quad s \in \{2, 3\}; \quad \bar{s} = \begin{cases} 3, & s = 2 \\ 2, & s = 3 \end{cases}$$

TABLE 5.2

INTERFERENCE INTEGRALS FOR MINIMAL SPACING

I Subinterval	$\frac{\pi}{2T}\int_I \cos((\nu_s - \omega_3)t - \nu_s\tau + \theta)dt$
$[0,\tau)$	$G_1(s,3) = \dfrac{\sin(\nu_s\tau - \theta) - \sin(\omega_3\tau - \theta)}{k + s - 3}$
$[\tau,2T)$	$G_2(s,3) = \dfrac{\sin(\omega_3\tau - \theta) + (-1)^{k+s}\sin(\nu_s\tau - \theta)}{k + s - 3}$

$$G(s,3) = G_1(s,3) + G_2(s,3) = \frac{(1 + (-1)^{k+s})\sin(\nu_s\tau - \theta)}{k + s - 3}$$

TABLE 5.3

COEFFICIENTS OF CROSSTALK FOR MINIMAL SPACING

Trigonometric Product Component of G	Case 0 G=G(s,3)	Case 1 $G=G_1(s,3)-G_2(s,3)$	Case 2 $G=G_1(s,3)+G_2(\bar{s},3)$	Case 3 $G=G_1(s,3)-G_2(\bar{s},3)$
$\sin(\nu_o\tau-\theta)\cos\delta\tau$	$\frac{1+(-1)^{k+s}}{k+s-3}$	$\frac{1-(-1)^{k+s}}{k+s-3}$	$\frac{(k+\bar{s}-3)-(-1)^{k+s}(k+s-3)}{k(k-1)}$	$\frac{(k+\bar{s}-3)+(-1)^{k+s}(k+s-3)}{k(k-1)}$
$\cos(\nu_o\tau-\theta)\sin\delta\tau$	$-\frac{(-1)^s+(-1)^k}{k+s-3}$	$-\frac{(-1)^s-(-1)^k}{k+s-3}$	$-\frac{(-1)^k(k+s-3)+(-1)^s(k+\bar{s}-3)}{k(k-1)}$	$\frac{(-1)^k(k+s-3)-(-1)^s(k+\bar{s}-3)}{k(k-1)}$
$\sin(\omega\tau_o-\theta)\cos\delta\tau$	0	$-\frac{2}{k+s-3}$	$\frac{2s-5}{k(k-1)}$	$\frac{-2k+1}{k(k-1)}$
$\cos(\omega_o\tau-\theta)\sin\delta\tau$	0	$-\frac{2}{k+s-3}$	$\frac{2s-5}{k(k-1)}$	$\frac{-2k+1}{k(k-1)}$

of Table 5.3 the worst-case crosstalk magnitude is

$$|G|_{max} = \left\{ \begin{array}{ll} \frac{4}{k-1} & , k \text{ odd} \\ \frac{2(2k-1)}{k(k-1)} & , k \text{ even} \end{array} \right\} , \quad k = 2, 3, 4, \ldots \quad . \tag{5.5}$$

5.2 Double Spacing

Now suppose the frequency spacing of Fig. 5.2 is doubled to 4δ with k_ν becoming 11, 13, 15,..., or k = 4, 5, 6,... to give a user bandwidth comparable to that for CPQFSK. The situation is summarized in Tables 5.4 and 5.5 with the worst-case crosstalk magnitude

$$|G|_{max} = \left\{ \begin{array}{ll} \frac{4}{k-2} & , k \text{ even} \\ \frac{4(k-1)}{k(k-2)} & , k \text{ odd} \end{array} \right\} , \quad k = 4, 5, 6, \ldots \quad . \tag{5.6}$$

With Eqs. (5.5) and (5.6) and normalizing, the worst-case crosstalks become

$$S_k(A, 1) = \left\{ \begin{array}{ll} \frac{4A}{\pi(k-1)} & , k \text{ odd} \\ \frac{2(2k-1)A}{\pi k(k-1)} & , k \text{ even} \end{array} \right\} \begin{array}{l} \text{minimal spacing} \\ , k = 2, 3, 4, \ldots \end{array} \tag{5.7a}$$

$$S_k(A, 1) = \left\{ \begin{array}{ll} \frac{4A}{\pi(k-2)} & , k \text{ even} \\ \frac{4(k-1)A}{\pi k(k-2)} & , k \text{ odd} \end{array} \right\} \begin{array}{l} \text{double spacing} \\ , k = 4, 5, 6, \ldots \quad . \end{array} \tag{5.7b}$$

Note that in all the above instances $S_k(A, 1) \sim 4A/\pi k$.

TABLE 5.4

INTERFERENCE INTEGRALS FOR DOUBLE SPACING

I Subinterval	$\frac{\pi}{2T}\int_I \cos((\nu_s - \omega_3)t - \nu_s\tau + \theta)dt$
$[0,\tau)$	$G_1(s,3) = \frac{\sin(\nu_s\tau - \theta) - \sin(\omega_3\tau - \theta)}{k + 2(s-3)}$
$[\tau,2T)$	$G_2(s,3) = \frac{\sin(\omega_3\tau - \theta) - (-1)^k\sin(\nu_s\tau - \theta)}{k + 2(s-3)}$

$$G(s,3) = G_1(s,3) + G_2(s,3) + \frac{(1-(-1)^k)\sin(\nu_s\tau - \theta)}{k + 2(s-3)}$$

TABLE 5.5

COEFFICIENTS OF CROSSTALK FOR DOUBLE SPACING

Trigonometric Product Component of G	Case 0 $G=G(s,3)$	Case 1 $G=G_1(s,3)-G_2(s,3)$	Case 2 $G=G_1(s,3)+G_2(\bar{s},3)$	Case 3 $G=G_1(s,3)-G_2(\bar{s},3)$
$\sin(\nu_o\tau-\theta)\cos 2\delta\tau$	$\frac{1-(-1)^k}{k+2(s-3)}$	$\frac{1+(-1)^k}{k+2(s-3)}$	$\frac{k+2(\bar{s}-3)-(-1)^k(k+2(s-3))}{k(k-2)}$	$\frac{k+2(\bar{s}-3)+(-1)^k(k+2(s-3))}{k(k-2)}$
$\cos(\nu_o\tau-\theta)\sin 2\delta\tau$	$\mp\frac{1-(-1)^k}{k+2(s-3)}, s=2,3$	$\mp\frac{1+(-1)^k}{k+2(s-3)}, s=2,3$	$\mp\frac{k+2(\bar{s}-3)+(-1)^k(k+2(s-3))}{k(k-2)}, s=2,3$	$\mp\frac{k+2(\bar{s}-3)-(-1)^k(k+2(s-3))}{k(k-2)}, s=2,3$
$\sin(\omega_o\tau-\theta)\cos 2\delta\tau$	0	$-\frac{2}{k+2(s-3)}$	$\mp\frac{2}{k(k-2)}, s=2,3$	$-\frac{2(k-1)}{k(k-2)}$
$\cos(\omega_o\tau-\theta)\sin 2\delta\tau$	0	$-\frac{2}{k+2(s-3)}$	$\mp\frac{2}{k(k-2)}, s=2,3$	$-\frac{2(k-1)}{k(k-2)}$

VI. FUTURE WORK

Only modems that achieve the optimal bit error performance in AWGN (through antipodal signaling) have been considered in this report so far. Although the crosstalk performances of these schemes are useful for comparing the relative capabilities of several important communications structures, there undoubtedly exist modems with better crosstalk properties. A broader investigation of this issue is warranted for bandlimited communications systems where the anticipated signal-to-noise ratio margin is sufficiently large that an optimization with respect to E_b/N_o is not as important as in the power-limited situation. It is more appropriate to view crosstalk among interuser signals as the basic limitation and to optimize the modems in some sense with respect to the overall bandwidth consumed by the system. For instance, one could ask if there are better ways to detect the modulation schemes already discussed to reduce the crosstalk or the required bandwidth.*

In general, given a certain number of FDM waveforms and a tolerable crosstalk level, one is interested in determining the class of modems that minimizes system bandwidth, suitably defined. Stated another way, given a fixed bandwidth and a tolerable crosstalk level, what modem permits the largest number of in-band waveforms?

The purpose of this final section is to expand on these remarks and to offer some suggestions that could be used as a basis for future work in this area. First an attempt is made to intuitively justify the asymptotic behavior of the crosstalk formulas already obtained.

---

* Some progress has already been made in this direction in the companion report [2] to this study.

The crosstalk formulas for the continuous-phase FSK modems of this report are all inversely proportional to the square of the center frequency separation between the two waveforms, i.e., $S_k(A,\lambda) = O(k^{-2})$ for MSK and CPQFSK. For all the other modems considered this dependence is only linear in the center frequency separation, i.e., $S_k(A,\lambda) = O(k^{-1})$ for BPSK, QPSK, AQPSK, SQPSK and biorthogonal FSK. This behavior is attributable to the fact that the MSK and CPQFSK waveforms are continuous while the waveforms of the other modulation schemes are discontinuous, allowing for arbitrary carrier phase. The spectrum of MSK and CPQFSK therefore varies as ω^{-4} asymptotically while the other spectra vary only as ω^{-2}. Hence, the order of magnitude advantage in the continuous-phase FSK crosstalk formulas is not surprising.

The fact that the derivative of the transmitted peak switching continuous-phase FSK waveforms is also continuous, which implies an asymptotic spectral dependence of $O(\omega^{-6})$, did not result in an $O(k^{-3})$ dependence as one might expect. This point may be just a consequence of the arbitrary phase θ in the crosstalk model of this report but deserves further attention. It is noted that the crosstalk formulas depended only on the differences of trigonometric arguments. Thus, the continuous-phase FSK waveforms need not be restricted to the peak switching form to achieve the $O(k^{-2})$ behavior. Similarly, although zero-crossing switching can be achieved with a restricted θ for BPSK or biorthogonal FSK (but just one component in each variant of QPSK), this signal continuity and the implied $O(k^{-2})$ dependence is destroyed for arbitrary θ.

It is also informative to examine the continuity properties of the modulating waveforms. With this purpose a family of modulation schemes containing SQPSK and MSK is defined.

Offset QPSK and MSK are the first two representatives of an infinite class of modulation schemes than can be detected on a binary antipodal signal basis. The (m + 1)-st member of the class is defined by the waveform

$$\pm \sin^m \delta t \sin \omega_o t \pm \cos^m \delta t \cos \omega_o t, \quad m = 0, 1, 2, \ldots$$

where the first term may change sign at t = 2nT while the second term may change sign at t =(2n − 1)T, n = 0, ± 1, ± 2, $\cdots$. By now an optimal (in AWGN) coherent receiver for detecting the binary antipodal signals of such a waveform should be obvious. SQPSK (m = 0) and MSK (m = 1) are both constant envelope schemes. The third (m = 2) member of the class employs raised-cosine modulation shaping on each channel [11] since

$$\sin^2 \delta t = \frac{1}{2} (1 - \cos 2\delta t) = \frac{1}{2} (1 + \cos 2\delta (t - T))$$

for $\delta = \pi/2T$. Note that the envelope

$$\sqrt{(\sin^m \delta t)^2 + (\cos^m \delta t)^2}\Big|_{m=2} = \sqrt{1 - \frac{1}{2} \sin^2 2\delta t}$$

is not constant for m = 2, but varies between 1 and $1/\sqrt{2}$.

A partial crosstalk calculation for this raised-cosine shaping has shown that the worst-case formula will vary as only k^{-1}, i.e., inversely with the center frequency separation. This behavior is governed by the constant part of the $\sin^2 \delta t$ above, or the rectangular component shaping reminiscent of the

m = 0 SQPSK case. The m = 2 case is interesting because it provides a counter-example to the tempting conjecture that crosstalk will decrease with an increase in the order of continuity of the modulation waveform. That is, one can observe that the modulation waveform is discontinuous for m = 0 and continuous for m = 1, while the SQPSK crosstalk is much larger than that for MSK. Even though the modulation has a continuous derivative for m = 2, the raised-cosine crosstalk is of the same asymptotic order as SQPSK. Thus, such a conjecture would be false.

Since the MSK crosstalk formulas are so promising, an intriguing question is whether one can find an optimal modulation waveshape s(t) for use in the more generalized offset quadrature-keying waveform

$$\pm\, s(t)\, \sin\omega_o t \pm s(t - T)\, \cos\omega_o t \quad .$$

Ideally, s(t) would be selected to minimize the crosstalk or bandwidth subject to an energy constraint. Though the modulation would probably not have a constant envelope, antipodal signal detection could still be employed. If this problem can be precisely formulated and solved it would be interesting to see how close the sinusoidal shaping $\sin\delta t$ of MSK is to the optimal s(t). Perhaps it can be shown that $\sin\delta t$ is an optimal shape for this form of offset keying.

Still more generally, an M-ary offset keying waveform

$$a_n\, s(t)\, \sin\omega_o t + b_n\, s(t - T)\, \cos\omega_o t$$

could be investigated. Here a_n assumes one of the values $\pm$ 1, $\pm$ 3,..., $\pm$ (K-1), K = 2, 4, 6,..., with transitions at t = 2nT, n = 0, $\pm$ 1, $\pm$ 2,$\cdots$. Similarly, b_n assumes one of the 2(K-1) amplitude values at t = (2n $-$ 1)T. For a fixed

modulating shape s(t), there are $M = K^2$ possible modulating signals. Note that offset M-ary quadrature amplitude-shift-keying (offset QASK-M; offset QASK-4 is equivalent to SQPSK) [12] is a special case when s(t) = 1. Of course, MSK is a special case when K = 2 and $s(t) = \sin\delta t$.

Departing from the realm of offset keying, there are other possibilities that may be worth pursuing. A comparison of the CPQFSK and MSK crosstalk formulas and the realization that M-ary FSK usually requires more bandwidth than M-ary PSK tends to discourage any further consideration of higher-order FSK modulation. However, M-ary PSK could be advantageous.

Just as QPSK is becoming more popular than BPSK because of the 50% savings in zero-crossing bandwidth with no sacrifice in bit error performance, higher-order PSK systems would result in a further reduction in bandwidth. If M is a power of two the zero-crossing bandwidth of MPSK is $2R/\log_2 M$, where R is the data rate. Parenthetically, it should be observed that the zero-crossing bandwidth of MSK is only 3R/2 [13]. Although the degradation in performance for 8PSK and 16PSK is substantial with respect to the required E_b/N_o in AWGN, cf. Fig. 6.1, the use of 8PSK or 16PSK may still be justifiable from a crosstalk point of view. Hence, crosstalk formulas for M-ary PSK modems were computed as sketched in the Appendix.

The main result is that for any M the worst-case crosstalk formula for MPSK is proportional to only the inverse of the center frequency separation.

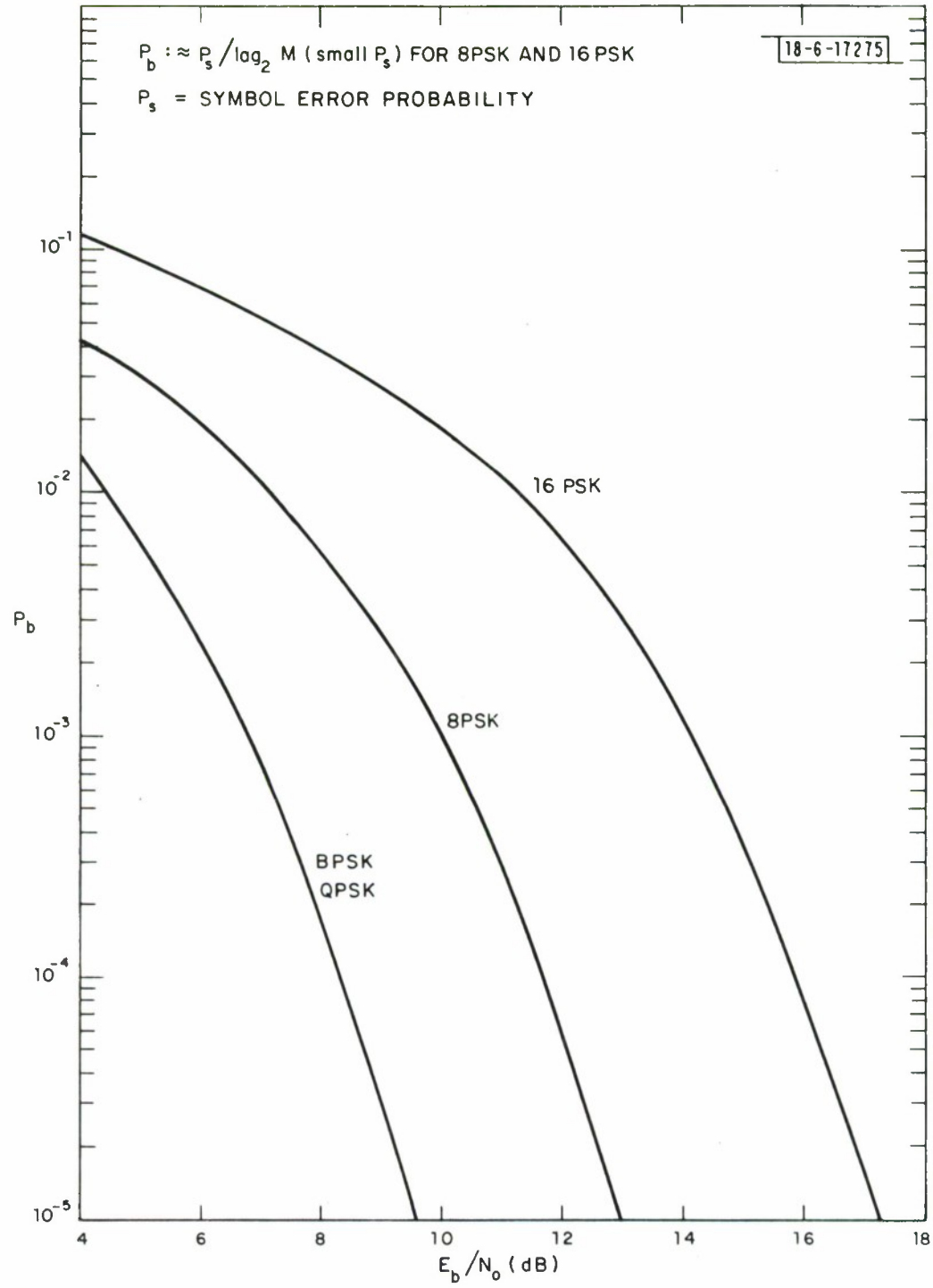

Fig. 6.1. Performance of coherent M-ary PSK in additive white Gaussian noise.

Furthermore, for an interesting example of relative SNR loss due to an unsynchronized interfering waveform, MSK requires a separation of only 2.5 R while MPSK requires 7.333 R for M = 8 and 5.5 R for M = 16. Thus, MPSK does not appear to be very attractive from a close packing viewpoint without additional spectral shaping, as suggested in the companion report [2].

Finally, let it be reiterated that every crosstalk formula of this report was computed assuming a particular set of discrete center frequency spacings between the two user signals given a fixed data rate R. The corresponding formulas that would result from a continuum of center frequency spacings should not be markedly different. That is, one should be able to treat the k of the crosstalk formulas as a continuous variable in a system design without introducing a significant change in the SNR degradation to be expected. However, because of the large number of crosstalk computations involved, estimates of these SNR variations will be deferred.

APPENDIX

CALCULATION OF M-ARY PSK CROSSTALK FORMULAS

Signal: $e^{j(\omega t + \psi)}$

ψ may change among M equally spaced phases every symbol interval
$T_s = T_{\log_2 M}$ (M power of two)

$r(t) = e^{j(\omega t + \psi)} + Ae^{j(\nu(t - \tau) + \phi + \theta)}$

$0 \leq \tau < T_s$ relative delay; θ relative phase

Demodulation: $\int_0^{T_s} r(t)e^{-j\omega t}dt$ and take ψ closest to phase of result

$$= T_s e^{j\psi} + \frac{Ae^{-jv}}{j\Delta}\left(e^{j\phi}(e^{j\Delta\tau}-1) + e^{j\phi'}(e^{j\Delta T_s} - e^{j\Delta\tau})\right)$$

where $\Delta = \nu - \omega$ $\quad v = \nu\tau - \theta$ $\quad w = \omega\tau - \theta$

$= w + \Delta\tau$

and where ϕ and ϕ' are the signaling phases of the interfering waveform for $0 \leq t < \tau$ and $\tau \leq t < T_s$, respectively.

Zero crosstalk when $\tau = 0$ implies $\Delta T_s \equiv 0 \pmod{2\pi}$; thus the

Relative crosstalk: $\frac{Ae^{-jv}}{j\Delta T_s e^{j\psi}}(e^{j\Delta\tau} - 1)(e^{j\phi} - e^{j\phi'})$

Clearly, $\Delta T_s = 2\pi k'$, $k' = 1,2,3,\cdots$, and if there is no phase change at τ in the interfering waveform, there is no crosstalk.

Assuming M even, the worst-case crosstalk occurs when $\Delta\tau \equiv \pi \pmod{2\pi}$ and when $\phi' \equiv \phi + \pi \pmod{2\pi}$; then the relative crosstalk is

$$\frac{4Ae^{-j(v-\phi)}}{j\Delta T_s e^{j\psi}} = -\frac{2Ae^{j(\phi-\psi-v)}}{j\pi k'}, \quad k'=1,2,3,\cdots .$$

Comparing MSK and MPSK for fixed relative crosstalk magnitude of $C_{max} = 11A/(120\pi)$ (see Table 1.1 for MSK with k = 10 and center frequency spacing $\Delta f = 2.5\ R$):

For MPSK must have: $C_{max} = \frac{2A}{\pi k'}$, $k=1,2,3,\cdots$

Solving yields $k' = 12$

Required $\Delta f = \frac{\Delta}{2\pi} = \frac{22}{T_s} = \frac{22R}{\log_2 M}$

$= 22\ R$ for $M = 2$

$= 11\ R$ for $M = 4$

$\doteq 7.333\ R$ for $M = 8$

$= 5.5\ R$ for $M = 16$.

MSK requires a spacing of only 2.5 R.

GLOSSARY

Abbreviations

AQPSK	alternating quadriphase shift keying
AWGN	additive white Gaussian noise
BPSK	binary phase shift keying
CPFSK	continuous-phase frequency shift keying
CPQFSK	continuous-phase quadrifrequency shift keying
FDM	frequency division multiplexed
MSK	minimum shift keying
QPSK	quadriphase shift keying
SNR	signal-to-noise ratio
SQPSK	offset quadriphase shift keying

Symbols

A	relative amplitude of interfering waveform
C_{max}	worst-case crosstalk
δ	half the radial frequency separation for frequency shift keying
Δf	center frequency separation between the signal waveform and the interfering waveform ($\Delta f = kR/4$)
E_b	received signal waveform energy per information bit
k	integer specifying the center frequency separation Δf
$L_k(A,\lambda)$	signal-to-noise ratio loss in dB
λ	threshold parameter specifying the crosstalk exceedance level
N_o	single-sided noise power spectral density
ν, ν_o	center radial frequency of the interfering waveform
P_b	bit error probability
$P_b(\lambda)$	bit error probability conditional on λ
$P(\lambda)$	probability that the crosstalk exceeds λC_{max}
R	information rate in bits per second ($R = 1/T$)
$S_k(A,\lambda)$	crosstalk ($C_{max} = S_k(A, 1)$)
T	$1/R$

θ	relative phase of interfering waveform
τ	relative delay of interfering waveform
ω, ω_o	center radial frequency of the signal waveform

Notations

:= (=:)	defines symbol on the left (right)
$\doteq$	approximation by rounding
$\sim$	asymptotic equality
$\equiv$	congruence (modular equality)
$\bullet \Big\vert_{m=2}$	$\bullet$ evaluated for m = 2
13+	number slightly larger than 13
O	asymptotic order ($x_k = O(k^{-1})$ implies $x_k \leq Mk^{-1}$ for some constant M)
$[\alpha,\beta)$	real interval $\alpha \leq x < \beta$
$\lfloor \bullet \rfloor$	largest integer no larger than $\bullet$

ACKNOWLEDGMENTS

S. L. Bernstein motivated this work with a calculation of the worst-case crosstalk for BPSK. B. Reiffen provided several stimulating ideas related to the asymptotic behavior of crosstalk formulas and the optimization of modems. S. L. Bernstein, K. S. Schneider and C. H. Moulton contributed to the simplification of CPQFSK receivers. C. H. Moulton also supplied computational support. I. Richer suggested the AQPSK form of modulation which can be useful for symbol timing acquisition because of the guaranteed $\pm$ 90° phase shifts. The author wishes to thank these colleagues for their interest and help.

REFERENCES

[1] B. Reiffen et al., "A Tentative Design for LES-10," Technical Note 1974-36, Lincoln Laboratory, M.I.T. (3 June 1974), DDC AD-919548-L.

[2] R. M. Mersereau and B. E. White, "A Bandwidth Conserving Approach to Multiple Access Satellite Communication for Mobile Terminals," Technical Note 1975-26, Lincoln Laboratory, M.I.T. (17 December 1975).

[3] J. M. Wozencraft and I. M. Jacobs, Principles of Communications Engineering (Wiley, New York, 1965), pp. 248-252.

[4] S. A. Rhodes, "Performance of Offset-QPSK Communications with Partially-Coherent Detection," Proc. 2nd IEEE National Telecommunications Conference, Atlanta, Georgia, 26-28 November 1973 ,pp. 32A1-32A8; also with different title, IEEE Trans. Commun. COM-22, 1046-1055 (1974).

[5] H. R. Mathwich, J. F. Balcewicz and M. Hecht, IEEE Trans. Commun. COM-22, 1525-1540 (1974).

[6] W. R. Bennett and J. R. Davey, Data Transmission (McGraw-Hill, New York, 1965), pp. 204-208.

[7] R. W. Lucky, J. Salz and E. J. Weldon, Principles of Data Communication (McGraw-Hill, New York, 1968), pp. 247-248.

[8] W. R. Osborne and M. B. Luntz, IEEE Trans. Commun. COM-22, 1023-1036 (1974).

[9] T. A. Schonhoff, "Symbol Error Probabilities for M-ary Coherent Continuous Phase Frequency-Shift Keying (CPFSK)," Proc. 11th IEEE International Conference on Communications, San Francisco, California, 16-18 June 1975, pp. 34-5 to 34-8.

[10] F. Chethik, "Analysis and Tests of Quadrature Advance/Retard Keying Modulation and Detection," Proc. 11th IEEE International Conference on Communications, San Francisco, California, 16-18 June 1975, pp. 21-21 to 21-25.

[11] S. A. Rhodes, "Effects of Hardlimiting on Bandlimited Transmissions with Conventional and Offset QPSK Modulation," Proc. 1st IEEE National Telecommunications Conference, Houston, Texas, 4-6 December 1972, pp. 20F1-20F7.

[12] M. K. Simon and J. G. Smith, IEEE Trans. Commun. COM-22, 1576-1584 (1974).

[13] B. E. White, IEEE Trans. Commun. Technol. COM-19, 536-539 (1971).

External Distribution List

The Defense Documentation Center
Attn: TISIA-1
Cameron Station, Bldg. 5
Alexandria, Virginia 22314 (2 copies)

Chief of Naval Operations (OP 941E)
Department of Navy
Washington, D. C. 20350

Computer Sciences Corporation
Systems Division 6565 Arlington Blvd.
Falls Church, Virginia 22046
Attn: Mr. C. C. Ingram
Mr. J. Burgess

Defense Communications Agency
8th and South Courthouse Road
Arlington, Virginia 22204
Attn: Dr. Frederick Bond
Dr. E. V. Hoversten
Dr. I. L. Lebow

Naval Electronics Laboratory Center
San Diego, California 92152
Attn: R.U.F. Hopkins Code 2420
Attn: Library

U.S. Naval Underwater Systems Center
New London Laboratory
Ft. Trumbull
New London, Connecticut 06321
Attn: Mr. John Merrill

Naval Postgraduate School
Electrical Engineering Dept.
Monterey, California 93940
Attn: Prof. John Ohlson, Code 52
Attn: Library

Commander
Naval Electronics Systems Command
Department of the Navy
Washington, D. C. 20360
Attn: PME-117
Attn: PME-106
Attn: PME-106-1, Capt. J. Pope
Attn: PME-106-1, Lt. Cdr. G. Burman
(6 copies)

NESC (continued)
Attn: PME-106-1, Lt. Cdr. G. J. Waylan
Attn: PME-106-1, J. Nooney
Attn: ELEX-03, T. B. Hughes
Attn: ELEX-00B, Dr. J. Lawson

U.S. Naval Research Laboratory
4555 Overlook Avenue, S. W.
Washington, D. C.
Attn: Code 5370, Mr. G. Goodman
Attn: Code 5400
Attn: Code 5404, Dr. W. S. Ament
Attn: Code 5406, Cdr. N. L. Wardle
Attn: Code 5430, Mr. Leavitt
Attn: Code 5430, Dr. LeFande

Department of the Navy
Command Support Programs, OP-094H
Washington, D. C. 20350
Attn: Dr. R. Conley

Department of the Navy
Naval Telecommunication Division
OP-941T
4401 Massachusetts Avenue
Washington, D. C. 20350
Attn: Dr. McAllister

Department of the Navy
Naval Telecommunication Systems
Architect, OP-941N
4401 Massachusetts Avenue
Washington, D. C. 20350

Joint Tactical Communication Office (TRI-TAC)
Code TT-E-EX
Fort Monmouth, New Jersey 07703
Attn: Lt. Col. Ralph Maruca, Jr.

Director, Telecommunication & Command
& Control Systems (D/TACCS)
Pentagon, 3D-161
Washington, D. C.
Attn: Dr. K. L. Jordan
Attn: Mr. G. Salton
Attn: Capt. R. Runyon
Attn: Dr. J. Neil Birch

Institute for Defense Analysis
400 Army Navy Drive
Arlington, Virginia 22202
Attn: Dr. J. Aein

Air Force Systems Command, XRTS
Andrews Air Force Base
Washington, D. C. 20331
Attn: Maj. A. BAker

Headquarters, U.S. Air Force, RDS
Pentagon Room 5D-320
Washington, D. C.
Attn: Lt. Col. J. Carpenter

U.S. Army Satellite Comm. Agency
Fort Monmouth, New Jersey 07703
Attn: D. L. Labanca

The MITRE Corporation
Bedford, Mass. 01730
Attn: W. T. Brandon

ESD/DCKS
Headquarters
L. G. Hanscom Field
Bedford, Mass. 01730

Defense Communications Eng. Center
Reston, Virginia
Attn: G. E. LaVean 22090

USAF-Avionics Laboratory
AFAL/AAI
Wright Patterson Air Force Base
Dayton, Ohio 45433

Dr. C. H. Chen
College of Engineering
Southeastern Mass. University
North Dartmouth, Mass. 02747

GTE Sylvania
77 "A" Street
Needham Heights, Mass. 02194
Attn: T. A. Schonhoff
J. H. Wittman
H. Gibbons

Biomedical Computer Laboratory
Washington University School of Medicine
700 S. Euclid Avenue
St. Louis, Missouri 63110

Electrical Engineering Department
Washington University-Box 1127
St. Louis, Missouri 63130
Attn: R. E. Morley, Jr.

Electrical Engineering Department
Massachusetts Institute of Technology
Cambridge, Massachusetts 02139
Attn: Prof. J. M. Wozencraft
Room 35-208

School of Electrical Engineering
Georgia Institute of Technology
Atlanta, Georgia 30328
Attn: Prof. R. M. Mersereau

REPORT DOCUMENTATION PAGE

READ INSTRUCTIONS BEFORE COMPLETING FORM

1. REPORT NUMBER: ESD-TR-75-283	2. GOVT ACCESSION NO.
3. RECIPIENT'S CATALOG NUMBER	
4. TITLE *(and Subtitle)*: On the Close Packing of Unsynchronized FDM Waveforms	5. TYPE OF REPORT & PERIOD COVERED: Technical Note
6. PERFORMING ORG. REPORT NUMBER: Technical Note 1975-34	
7. AUTHOR*(s)*: White, Brian E.	8. CONTRACT OR GRANT NUMBER*(s)*: F19628-76-C-0002
9. PERFORMING ORGANIZATION NAME AND ADDRESS: Lincoln Laboratory, M.I.T. P.O. Box 73 Lexington, MA 02173	10. PROGRAM ELEMENT, PROJECT, TASK AREA & WORK UNIT NUMBERS: Navy Project No. 2D123279
11. CONTROLLING OFFICE NAME AND ADDRESS: Naval Electronic Systems Command Department of the Navy Washington, DC 20360	12. REPORT DATE: 14 October 1975
	13. NUMBER OF PAGES: 102
14. MONITORING AGENCY NAME & ADDRESS *(if different from Controlling Office)*: Electronic Systems Division Hanscom AFB Bedford, MA 01731	15. SECURITY CLASS. *(of this report)*: Unclassified
	15a. DECLASSIFICATION DOWNGRADING SCHEDULE

16. DISTRIBUTION STATEMENT *(of this Report)*

Approved for public release; distribution unlimited.

17. DISTRIBUTION STATEMENT *(of the abstract entered in Block 20, if different from Report)*

18. SUPPLEMENTARY NOTES

None

19. KEY WORDS *(Continue on reverse side if necessary and identify by block number)*

close packing
FDM waveforms
frequency shift keying
crosstalk
communications satellite
mobile terminals

20. ABSTRACT *(Continue on reverse side if necessary and identify by block number)*

The effects of crosstalk on unsynchronized FDM communication links operating in the presence of additive white Gaussian noise are considered for several modulation schemes. Continuous-phase frequency shift keying is found to be far superior to various forms of phase shift keying in the sense that many more uncoordinated frequency division multiplexed waveforms can be packed into a given bandwidth for a certain imbalance in transmitter powers. This result can be applied to the uplinks and/or downlinks of a demodulating communications satellite serving a multitude of mobile terminals.